

Considerations on the Thermophysical Properties of Nanofluids

K.V. Sharma, Akilu Suleiman, Hj. Suhaimi B. Hassan
and Gurumurthy Hegde

Abstract The properties such as viscosity, thermal conductivity, specific heat, and density of nanofluids have been determined by various investigators through experiments. An equation developed for specific heat and density employing the law of mixtures is observed to be valid when compared with the experimental data. However, the experimental data of viscosity and thermal conductivity reported by investigators are observed to vary by more than 25 % for certain nanofluids. Theoretical models for the estimation of properties are yet to be developed. The nanofluid properties are essential for the comparison of heat transfer enhancement capabilities. Equations are developed for the estimation of viscosity and thermal conductivity by Corcione and Sharma et al. These equations are flexible to determine the nanofluid properties for a wide range of operating parameters which can predict the experimental data of water-based nanofluids with a maximum deviation of 12 %.

Keywords Water-based nanofluids · Nanofluid properties · Regression equations · Estimation of thermal conductivity and viscosity

Nomenclature

C	Specific heat at constant pressure, J/(K kg)
C_{RM}	Random motion velocity of nanoparticles, m/s
D	Diameter, nm
HR	Non-dimensional heat capacity ratio $[(\rho C)_p/(\rho C)_{nf}]$
H	Interparticle spacing
K	Thermal conductivity, J/(K m)

K.V. Sharma (✉) · A. Suleiman · Hj.S.B. Hassan
Mechanical Engineering Department, Universiti Teknologi PETRONAS,
32610 Bandar Seri Iskandar, Perak Darul Ridzuan, Malaysia
e-mail: kvsharmajntu@gmail.com

G. Hegde
BMS R&D Centre, BMS College of Engineering, Basavanagudi, Bangalore 560019, India

k_B	Boltzmann constant, 1.3807×10^{-23} J/K
k_{pe}	Equivalent thermal conductivity
L	Molecular weight of the base fluid
N	Avogadro's number
N	Empirical shape factor 'n' is equal to $3/\psi$
Pr	Prandtl number
R	Thermal resistance (K m ²)/W
R_b	Interfacial thermal resistance between nanoparticle and the fluid
Re	Reynolds number
r_m	Radius of the liquid species
r_p	Radius of the suspended particles
T	Thickness, m
T	Temperature, K or °C

Greek symbols

α	Thermal diffusivity, $[k/\rho C]$ (m ² /s)
β	Ratio of nanolayer thickness to the particle radius
ω	$= \left[\frac{d_p}{(d_p + 2t)} \right]^3$
\varnothing	Volume fraction of nanoparticles in per cent
ϕ_m	Maximum packing fraction
γ	Ratio of thermal conductivity of the layer to that of the particle
μ	Absolute viscosity, kg/(m s)
μ_r	Relative viscosity of the suspension
ϑ	Kinematic viscosity (m ² /s)
ρ	Density (kg/m ³)
ρ_{bf0}	Mass density of the base fluid calculated at 20 °C
fr	Freezing point of the base liquid
η	Intrinsic viscosity
ψ	Sphericity

Subscripts

bf	Base fluid
eff	Effective
i	Interface
nf	Nanofluid
neff	Net effective
w	Water
p	Nanoparticle

1 Introduction

Nanofluids are particle suspensions of metals, metal oxides, carbides, nitrides, carbon nanotubes, etc., dispersed in a continuous medium such as water, ethylene glycol, refrigerants, and engine oil of size less than 100 nm. The thermophysical properties of nanofluids are observed to be greater than those of the base liquids. Their use in industrial applications require the development of stable nanofluids with their properties determined.

The properties of stable nanofluids with metals such as copper, silver, gold, and oxides, namely Al_2O_3 , CuO , TiO_2 , SiO_2 , ZnO , and ZrO_2 , in water and ethylene glycol are widely investigated because of their potential as heat transfer fluid with applications for thermal energy transfer in automotive, solar, and cooling electronic appliances. Studies are undertaken to determine ways to stabilize nanofluids from agglomeration for long term applications. The thermophysical properties of nanofluids which are important for applications involving single phase convective heat transfer are viscosity, thermal conductivity, specific heat and density.

2 Viscosity Models

The earliest studies for the determination of viscosity of suspended particles in liquids were undertaken by Einstein. An equation has been proposed based on the liquid particle interaction, which can predict the effective viscosity of liquid for volume concentrations lower than 1.0 %. The Einstein's equation is given by Eq. (1):

$$\mu_r = \mu_{nf} / \mu_w = (1.0 + 2.5\phi) \tag{1}$$

Brinkman (1952) extended the validity of Einstein's equation up to 4.0 % volume concentration given by Eq. (2) as:

$$\mu_r = \mu_{nf} / \mu_w = 1 / (1 - \phi)^{2.5} \tag{2}$$

Krieger and Dougherty (1959) presented a semiempirical equation expressed as in Eq. (3):

$$\mu_r = \mu_{nf} / \mu_w = (1 - \phi / \phi_m)^{-[\eta]\phi_m} \tag{3}$$

where η is the intrinsic viscosity (2.5 for solid spheres) and ϕ_m is the maximum packing fraction. The maximum close-packing fraction is approximately 0.64 for randomly monodispersed spheres. Frankel and Acrivos (1967) proposed an equation for viscosity given by:

$$\mu_r = \frac{\mu_{nf}}{\mu_w} = \frac{9}{8} \left[\frac{(\varnothing/\varnothing_m)^{1/3}}{1 - (\varnothing/\varnothing_m)^{1/3}} \right] \quad (4)$$

where \varnothing_m is the maximum particle volume fraction determined from experiments. Nielsen (1970) proposed a different model for a low concentration of particles. Nielsen's equation is given by:

$$\mu_r = \mu_{nf}/\mu_w = (1 + 1.5\varnothing) \exp[\varnothing/(1 - \varnothing_m)] \quad (5)$$

where \varnothing and \varnothing_m are the volume fraction of particles and the maximum packing fraction, respectively. Lundgren (1972) proposed an equation developed in the form of Taylor series given by:

$$\mu_r = \mu_{nf}/\mu_w = 1 + 2.5\varnothing + \frac{25}{4}\varnothing^2 + O(\varnothing^3) \quad (6)$$

With increasing particle volume concentration, the flow around a particle is influenced by the neighbouring particles. Batchelor (1977) studied the effect of these hydrodynamic interactions or the Brownian motion on viscosity of suspensions and developed a relation valid for particle volume concentrations up to 10.0 % as:

$$\mu_r = \mu_{nf}/\mu_w = (1 + 2.5\varnothing + 6.2\varnothing^2) \quad (7)$$

where μ_r is the relative viscosity of the suspension and \varnothing is the volume fraction. Graham (1981) proposed a generalized form of Frankel and Acrivos (1967) formula that agrees well with Einstein's equation for small values of volume concentration. The equation developed is:

$$\mu_r = \mu_{nf}/\mu_w = 1 + 2.5\varnothing + 4.5/\left(\frac{h}{d_p}\right) \left(2 + \frac{h}{d_p}\right) \left(1 + \frac{h}{d_p}\right)^2 \quad (8)$$

where d_p is the particle diameter and h is the interparticle spacing. A simple expression was proposed by Kitano et al. (1981) by involving maximum particle volume concentration term \varnothing_m to predict the viscosity of nanofluids:

$$\mu_r = \mu_{nf}/\mu_w = (1 - \varnothing/\varnothing_m)^{-2} \quad (9)$$

The White (1991) formula estimates the viscosity of water considering the effect of temperature given by:

$$\ln\left(\frac{\mu_{bf}}{\mu_o}\right) \approx a + b\left(\frac{T_o}{T}\right) + c\left(\frac{T_o}{T}\right)^2 \quad (10)$$

where μ_o, T_o are the reference values and $a = 2.10$, $b = 4.45$, and $c = 6.55$. The most referred equation on dynamic viscosity of water with the influence of temperature is given by Hagen (1999) as follows:

$$\mu_{bf} \times 10^4 = \exp[(1.12646 - 0.039638T)/(1 - 0.00729769T)] \quad (11)$$

The data of Wang et al. (1999) have been regressed by Duangthongsuk and Wongwises (2009) with less than 1 % deviation for the determination of Al₂O₃/water nanofluid viscosity given by:

$$\mu_r = \mu_{nf} / \mu_w = (1 + 7.3\phi + 123\phi^2) \quad (12)$$

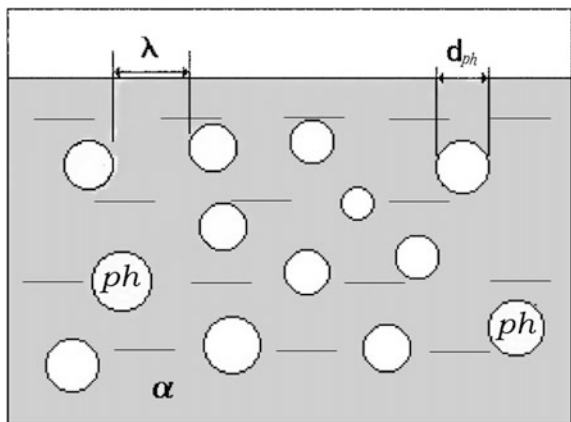
Depending on the physical state of the phases, e.g. solid–solid or solid–liquid, different forms of representing concentration are convenient. In a solid–liquid system, the volume fraction of a phase is usual. In a solid–solid system, the Fullman model for the mean free path λ shown in Fig. 1 can be used to indicate the average distance between two particles of phase ph. Based on the mean free path λ of the nanoparticles in the base fluid, Noni et al. (2002) proposed a correlation which is given as:

$$\mu_{nf} / \mu_w = 1 + c \frac{1}{\lambda^n} \quad (13)$$

where an average distance between two particles of phase ph having an average size d_{ph} in a matrix of phase α and $\lambda = \frac{2}{3} d_{ph} \left(\frac{1 - \phi_{ph}}{\phi_{ph}} \right)$ given by Fullman (1953),

ϕ_{ph} is the volume fraction of phase in the system,
 d_{ph} is the average diameter of phase,
 ‘c’ and ‘n’ are constants.

Fig. 1 A typical two-phase system



Tseng and Lin (2003) developed viscosity correlation for TiO₂ nanoparticles (7–20 nm) suspended in distilled water in the particle concentration from 0.05 to 0.12 % with a correlation factor $R^2 = 0.98$ which is given as:

$$\mu_{nf}/\mu_w = 13.45 \exp(35.98\phi) \quad (14)$$

Chen et al. (2007) modified the Krieger–Dougherty (1959) equation by considering $\phi = (a_a/a)^{3-D}$

$$\mu_r = \mu_{nf}/\mu_w = \left(1 - \frac{\phi}{\phi_m} \left(\frac{a_a}{a}\right)^{1.2}\right)^{-[\eta]\phi_m} \quad (15)$$

where a_a and a are the radii of aggregates and primary nanoparticles, respectively. The term D is defined as the fractal index, which for nanoparticles has a typical value of 1.8 given by Chen et al. (2007). Review articles are presented by Ghadimi et al. (2011), Mahbubul et al. (2012), Sundar et al. (2013), Mishra et al. (2014), and Sharma et al. (2016) covering theoretical and experimental works.

2.1 Experimental Determination of Viscosity

The experimental determination of nanofluid viscosity was undertaken by Pak and Cho (1998) who observed Newtonian behaviour with Al₂O₃ of size 13 nm and TiO₂ of size 27 nm for particle volume concentration lower than 3 and 10 %, respectively. The fluids showed shear thinning behaviour (i.e. decrease in viscosity with shear rate) indicating non-Newtonian behaviour at higher volume concentrations. They showed that the Bachelor's model failed to predict the viscosity of the nanofluids, although the volume fraction of the particles is within the range of applicability.

Junming et al. (2002) have measured the viscosity of CuO nanoparticles dispersed in water with the particle concentration range of 2–10 % and in the temperature range of 30–80 °C. The viscosity of the suspensions was reported to be higher than that of water by 15–30 %.

Prasher et al. (2006) have performed experiments to determine the viscosity of Al₂O₃-based nanofluids and pure propylene glycol at various temperatures (30–60 °C), nanoparticle diameter (27, 40, and 50 nm), and nanoparticle volume fraction (0.5–3 %). The viscosities of pure propylene glycol (PG) at 20 and 40 °C were found to be 0.0629 and 0.02 Pa s, respectively.

Kulkarni et al. (2006) conducted experiments to determine the rheological behaviour of copper oxide (CuO) nanoparticles having an average diameter of 29 nm, dispersed in deionized (DI) water, over a range of volume concentrations between 5 and 15 % and temperatures varying between 278 and 323 K. Their work

yielded a well-developed generalized correlation for liquid viscosity given by Eq. (16):

$$\ln \mu_s = A(1/T) - B \tag{16}$$

where μ_s is the suspension viscosity and A and B are polynomials which are functions of particle volumetric concentrations. These factors are given as:

$$A = 20587\phi^2 + 15857\phi + 1078.3\phi^3 \quad \text{with } R^2 = 0.99$$

$$B = -107.12\phi^2 + 53.548\phi + 2.8715 \quad \text{with } R^2 = 0.97$$

where ϕ is the volume fraction ranging from 0.05 to 0.15.

Calculated values from the above equation and the experimental values were compared, and these values are within $\pm 10\%$, except for two data points at temperatures 278 and 283 K, for a 15% CuO suspension.

Kulkarni et al. (2007) have studied the rheological properties of CuO nanoparticles dispersed in PG and water in the ratio of 60:40 by weight in the temperature range of -35 to 50 °C in particle concentration range of 0–5.9%. The experimental data of base fluid without any particle suspension and nanofluid were compared with ASHRAE data (2005) and Batchelor’s equation (1977), respectively, and it was observed to show good agreement with ASHRAE data for the former, whereas the latter shows substantial deviation from the equation. A correlation has been developed for the nanofluid given by:

$$\mu_s = Ae^{B\phi} \tag{17}$$

where the factors A and B are correlated as:

$$\ln(A) = 736.9 \exp(-0.0199T) \quad \text{with } R^2 = 0.99$$

$$B = 44.794 - 0.0765T \quad \text{with } R^2 = 0.99$$

The deviation between experimental data and values given by this correlation is reported to be within $\pm 10\%$. Nguyen et al. (2007) conducted experiments for the determination of viscosity of Al_2O_3 and CuO nanofluids in water at different concentrations, particle sizes, and a temperature range of 22–75 °C. Experiments with Al_2O_3 having particle sizes of 36 and 47 nm and CuO with 29 nm size revealed a strong dependence of viscosity on volume concentration of the nanofluid. The viscosity is not significantly influenced by the particle size for concentration less than 4.0%. They presented equations for the determination of dynamic viscosity of Al_2O_3 and CuO nanofluid based on concentration for 1.0 and 4.0%, respectively, as:

$$\mu_r = \mu_{nf}/\mu_w = (1.1250 - 0.0007T) \quad (18)$$

$$\mu_r = \mu_{nf}/\mu_w = (2.1275 - 0.0215T + 0.0002T^2) \quad (19)$$

Lee et al. (2008) conducted experiments for a maximum volume concentration of 0.3 % with 30 nm Al_2O_3 particles dispersed in deionized water in the temperature range of 21–39 °C. Duangthongsuk and Wongwises (2009) conducted experiments with TiO_2 (21 nm) nanoparticles dispersed in water in the volume concentration of 0.2–2.0 % for temperatures varying between 15 and 35 °C. They developed Eq. (12) using the experimental data of Wang et al. (1999).

Turgut et al. (2009) undertook experiments to determine the viscosity of TiO_2 (21 nm) nanoparticles in deionized water for volume concentration up to 3 % and in the temperature range of 13–55 °C. It is reported that the increase in viscosity is greater than the values predicted with Einstein model.

Namburu et al. (2007) conducted experiments to compare the viscosity of SiO_2 (20, 50, and 100 nm) nanoparticles suspended in ethylene glycol (EG) and water mixture in the ratio of 60:40 by weight in the concentration range of 0–10 % and temperature of –35 to +50 °C. It is observed that SiO_2 nanofluid dispersed with 100-nm-sized particles at 8 % concentration has the lowest viscosity. Godson et al. (2010) in their article detailed their experiments to determine the viscosity of silver (Ag) nanofluid in DI water in the range of 0.3–0.9 % volume concentration and temperature of 50–90 °C. The effect of Brownian motion and thermophoresis on the thermophysical properties is discussed. An experimental correlation for viscosity relating the volume concentration and temperature is developed. The correlation between Eqs. (20) and (21) is reported to be in good agreement with the experimental data.

$$k_{nf}/k_w = (0.9692\phi + 0.9508) \quad (20)$$

$$\mu_{nf}/\mu_w = (1.005 + 0.497\phi - 0.1149\phi^2) \quad (21)$$

Experiments are conducted for the determination of nanofluid viscosity prepared by dispersing Al_2O_3 nanoparticles of size <50 nm for application as a coolant in a commercial vehicle by Kole and Dey (2010). The experiments are conducted in the temperature range of 10–80 °C. Newtonian behaviour is observed for nanofluid at volume concentrations lower than 4 % and non-Newtonian behaviour at higher concentrations in the range of temperature measured. An empirical correlation has been proposed by Kole and Dey (2010) given by:

$$\log(\mu_{nf}) = A \exp(-BT) \quad (22)$$

where

$$A = -225.245\varnothing^2 + 18.404\varnothing + 1.749 \text{ and}$$

$$B = 575.835\varnothing^3 - 32.101\varnothing^2 + 0.149\varnothing + 0.011$$

Corcione (2011) proposed an empirical correlation for the nanofluid effective dynamic viscosity. It was derived from a wide selection of experimental data available in the literature consisting of Al_2O_3 , TiO_2 , SiO_2 , and Cu nanoparticles with diameters in the range of 25–200 nm, suspended in water, ethylene glycol, propylene glycol, and ethanol. The best fit of regression analysis with 1.84 % deviation as:

$$\mu_{\text{nf}}/\mu_{\text{w}} = 1/\left[1 - 34.87(d_{\text{p}}/d_{\text{bf}})^{-0.3}\varnothing^{1.03}\right] \quad (23)$$

where $d_{\text{bf}} = 0.1\left(\frac{6M}{N\pi\rho_{\text{bf0}}}\right)^{1/3}$ is the equivalent diameter of a base fluid molecule, in which M is the molecular weight of the base fluid, N is the Avogadro’s number, and ρ_{bf0} is the mass density of the base fluid calculated at 293 K. The equation is applicable for volume concentration up to 7.1 % in the temperature range of 293–333 K.

Sundar et al. (2014) undertook experimental investigation to determine the influence of EG/water-based liquid mixture ratios of 20:80, 40:60, and 60:40 % by weight, with Al_2O_3 nanoparticles, on viscosity in the temperature range of 20–60 °C. It is reported that a maximum enhancement ratio of 2.58 is obtained with nanofluid of 1.5 % concentration at a temperature of 0 °C with 60:40 % EG/water ratio as compared to base liquid.

Based on the studies undertaken by various investigators, the following observations can be deduced for nanofluids in base liquid water, EG, and EG/water mixtures.

- Newtonian behaviour is observed for volume concentration lower than 4 % in the temperature range of 20–70 °C.
- Viscosity increases with the increase in concentration of the nanofluid.
- Viscosity of the nanofluid decreases with the increase in temperature.
- Viscosity increases with the decrease in particle size which is observed by most of the investigators.
- Viscosity enhancement in base liquid EG is reported by many investigators to be higher than that with water.
- The nature of material may not have significant influence on nanofluid viscosity.

Based on the observations, an empirical equation has been presented by Sharma et al. (2010) as:

$$\mu_{\text{r}} = \frac{\mu_{\text{nf}}}{\mu_{\text{w}}} = C_1\left(1 + \frac{\varnothing}{100}\right)^{11.3}\left(1 + \frac{T_{\text{nf}}}{70}\right)^{-0.038}\left(1 + \frac{d_{\text{p}}}{70}\right)^{-0.061} \quad (24)$$

The value of C_1 is 1.0 for metal and metal oxide nanofluids. The value is 1.4 for SiC nanofluid. The data could be correlated with an average deviation of 3.18 %, standard deviation of 3.8 %, and a maximum deviation of 13 %.

3 Nanofluid Thermal Conductivity

Early studies devoted for the determination of effective thermal conductivity of nanofluid are based on the classical analysis of Maxwell (1881) for two-phase solid–liquid mixtures given by:

$$k_{\text{eff}} = k_{\text{bf}} \left[\frac{k_p + 2k_{\text{bf}} + 2\phi(k_p - k_{\text{bf}})}{k_p + 2k_{\text{bf}} - \phi(k_p - k_{\text{bf}})} \right] \quad (25)$$

The model makes satisfactory predictions for spherical shaped particles at low volume concentration ϕ and at ambient conditions. The limitation on the particle volume concentration proposed by Maxwell has been relaxed by Bruggemen (1935). The interactions among the randomly distributed particles is taken into consideration, and an equation has been proposed in implicit form given by:

$$\phi \left[\frac{k_p - k_{\text{eff}}}{k_p + 2k_{\text{eff}}} \right] + (1 - \phi) \left[\frac{k_p - k_{\text{eff}}}{k_p + 2k_{\text{neff}}} \right] = 0 \quad (26)$$

where k_{eff} is estimated using Eq. (25) and the net effective thermal conductivity k_{neff} of the two-phase fluid is determined.

Even though nanoparticles are many orders smaller than micron sized solid suspensions, modifications and addition of suitable terms and/or consideration of dynamic factors associated with nanofluids are made to Maxwell's model by the investigators. Various models are developed to predict the thermal conductivity of nanofluids as they exhibit higher thermal conductivity even at low concentrations of the suspended nanoparticles. Further information can be had from review articles of Das et al. (2006), Wang and Mujumdar (2007), Buongiorno et al. (2009), Kakaç and Pramuanjaroenkij (2009), Özerinç et al. (2010), Lee et al. (2010), Khanafer and Vafai (2011), Ghadimi et al. (2011), Sridhara and Satapathy (2011), Xie et al. (2011), and Kleinstreuer and Feng (2011).

3.1 Nanofluid Thermal Conductivity, k_{nf} Models

The equation of Hamilton and Crosser (1962) is widely used for comparison of the experimental data by various investigators. The equation for determining the nanofluid thermal conductivity is given by:

$$k_{nf} = k_{bf} \left[\frac{k_p + (n - 1)k_{bf} - \varnothing(n - 1)(k_{bf} - k_p)}{k_p + (n - 1)k_{bf} + \varnothing(k_{bf} - k_p)} \right] \quad (27)$$

where the empirical shape factor ‘ n ’ is equal to $3/\psi$ and ψ the sphericity. Sphericity is defined as the ratio of the surface area of a sphere with the volume equal to that of the average particle, to the surface area of the particle. The sphericity is 1.0 and 0.5 for spherical and cylindrical shapes. The model is valid as long as the conductivity of the particle is larger by a factor of 100 compared to that of the continuous phase. The Hamilton and Crosser model reduces to Maxwell’s model when $\psi = 1$ and is found to be in agreement with experimental data for $\varnothing < 30\%$. Equation (27) does not include the effect of particle size on thermal conductivity. The value of thermal conductivity predicted by this model is observed to be lower than the experimental values obtained from nanosized particles.

Wasp (1977) has given a correlation for determining the nanofluid k_{nf}

$$k_{nf} = k_{bf} \left[\frac{k_p + 2k_{bf} + 2(k_{bf} - k_p)\varnothing}{k_p + 2k_{bf} - (k_{bf} - k_p)\varnothing} \right] \quad (28)$$

A modification to the Maxwell model is proposed by Keblinski et al. (2002). According to Keblinski et al. (2002), it be due to (i) particle collisions occurring during Brownian motion, (ii) ordered atomic structure of liquid layer at the solid–liquid interface, (iii) propagation of heat due to lattice vibrations by phonons in random directions and (iv) rapid movement of heat in clusters formed by particles, contributing for the overall enhancement of nanofluid thermal conductivity.

Yu and Choi (2003) renovated the Maxwell model by considering the base fluid molecules close to the surface of the nanoparticles to form a solid-like nanolayered structure with thermal conductivity greater than the bulk fluid. The thermal conductivity of the solid particles and the nanolayer is combined to arrive at equivalent thermal conductivity k_{pe} of particle given by:

$$k_{pe} = k_p \left\{ \frac{\gamma \left[2(1 - \gamma) + (1 + \beta)^3(1 + 2\gamma) \right]}{-(1 - \gamma) + (1 + \beta)^3(1 + 2\gamma)} \right\} \quad (29)$$

where γ is the ratio of thermal conductivity of the layer to that of particle and β is the ratio of nanolayer thickness to the particle radius. The nanofluid thermal conductivity is estimated with the relation given by:

$$k_{nf} = k_{bf} \left[\frac{k_{pe} + 2k_{bf} + 2(k_{pe} - k_{bf})(1 + \beta)^3\varnothing}{k_{pe} + 2k_{bf} - (k_{pe} - k_{bf})(1 + \beta)^3\varnothing} \right] \quad (30)$$

The layer thermal conductivity is varied in the range of 10–100 k_{bf} , and layer thickness is in the range of 1–2 nm. The experimental thermal conductivity ratio of CuO nanofluid in base liquid ethylene glycol (EG) is observed to be in good

agreement with the values estimated with Eq. (30) in the concentration range of $0 < \phi < 5\%$ for a particle diameter of 30 nm. A maximum enhancement of 20 % is shown along with the experimental data of CuO nanofluid. Thermal conductivity enhancement of up to 90 % is predicted by Yu and Choi (2003) for 6-nm Cu nanoparticles dispersed in EG for an assumed layer thickness of 2 nm.

Xue (2003) developed a model based on Maxwell employing average polarization theory. The particle with its liquid interface termed ‘complex nanoparticle’ is considered to be dispersed in a base liquid. The predicted values of thermal conductivity ratio for $\text{Al}_2\text{O}_3/\text{water}$ are shown to vary linearly for ‘interfacial shell thickness’ in the range of 3–5 nm for nanofluid concentration of $0 < \phi < 5\%$.

$$9 \left(1 - \frac{\phi}{\omega} \right) \frac{k_{\text{eff}} - k_{\text{bf}}}{2k_{\text{eff}} + k_{\text{bf}}} + \frac{\phi}{\omega} \left[\frac{k_{\text{eff}} - k_{c,x}}{k_{\text{eff}} + B_{2,x}(k_{c,x} - k_{\text{eff}})} + 4 \frac{k_{\text{eff}} - k_{c,y}}{2k_{\text{nf}} + (1 - B_{2,x})(k_{c,y} - k_{\text{eff}})} \right] = 0 \quad (31)$$

In another paper, Yu and Choi (2004) modelled the thermal conductivity enhancement as due to liquid layering around a nanoparticle considering Hamilton–Crosser model. It is observed that the thermal conductivity of the interfacial layer k_i should be at least 100 times the value of k_p or k_{bf} in order to obtain an increase in the effective thermal conductivity for non-spherical particles. The authors compared the experimental values of CNT in oil to substantiate their observations. For spherical particles, the predicted value of k_{nf} is observed to increase with thickness or thermal conductivity of the interfacial layer.

Xie et al. (2005) solved the heat conduction equation in spherical coordinates with the consideration of interfacial liquid layer on nanoparticle. They related the nanofluid thermal conductivity to system parameters, viz. k_p , k_{pe} , k_i —volume fraction, size of nanoparticle, and thickness of the nanolayer. They compared the experimental data of $\text{Al}_2\text{O}_3/\text{water}$, CuO/EG, and Cu/EG nanofluid for concentrations up to 5.0 % with the results from their model. They assumed the nanolayer thermal conductivity to be 5 times that of the base liquid and reported good agreement with experimental data for 2 nm layer thickness.

A theoretical model having shells on the surface of the solid nanoparticles is proposed by Xue and Xu (2005). Based on the model, an implicit relation for the determination of nanofluid thermal conductivity is developed as:

$$\left(1 - \frac{\phi}{\omega} \right) \left[\frac{k_{\text{nf}} - k_{\text{bf}}}{2k_{\text{nf}} + k_{\text{bf}}} + \frac{\phi}{\omega} \frac{(k_{\text{nf}} - k_i)(2k_i + k_p) - \omega(k_p - k_i)(2k_i + k_{\text{nf}})}{(2k_{\text{nf}} - k_i)(2k_i + k_p) + 2\omega(k_p - k_i)(2k_i - k_{\text{nf}})} \right] = 0 \quad (32)$$

where $\omega = \left[\frac{d_p}{(d_p + 2r)} \right]^3$ and k_i is the thermal conductivity of the interfacial shell and ‘ r ’ represents the thickness of the shell which is different for different nanofluids.

The thickness of the shell is considered as 3 nm to obtain a value of $k_i = 5.0 \text{ W/mK}$.

The enhancement in nanofluid thermal conductivity is due to Brownian motion according to Jang and Choi (2004). They showed a good agreement of the experimental data of $\text{Al}_2\text{O}_3/\text{water}$, CuO/water , CuO/EG , and Cu/EG nanofluids with the results from their model.

A semiempirical correlation considering Brownian motion proposed by Chon et al. (2005) is given by Eq. (33). The authors showed a good agreement of the experimental data of Al_2O_3 nanofluid for different parameters with values estimated by using Eq. (33).

$$\frac{k_{\text{nf}}}{k_{\text{bf}}} = 1 + 64.7 \phi^{0.7460} \left(\frac{d_{\text{bf}}}{d_{\text{p}}} \right)^{0.3690} \left(\frac{k_{\text{p}}}{k_{\text{bf}}} \right)^{0.7476} Pr_{\text{bf}}^{0.9955} Re^{1.2321} \quad (33)$$

where d_{bf} is the molecular diameter of the base fluid, $Re = \frac{\rho_{\text{bf}} K_{\text{B}} T}{3\pi\mu_{\text{bf}}^2 l_{\text{bf}}}$ where $l_{\text{bf}} = 0.17 \text{ mm}$ the mean free path for water and Boltzmann constant $k_{\text{B}} = 1.3807e^{-23} \text{ J/K}$ used in their analysis.

Koo and Kleinstreuer (2004) proposed an equation for the determination of effective thermal conductivity of nanofluid which is modelled for combined influence of Maxwell and Brownian motion. It takes into account the effect of particle size, volume concentration, temperature, and properties of base fluid as well as nanoparticle subject to Brownian motion given by:

$$k_{\text{nf}} = k_{\text{bf}} \left[\frac{k_{\text{p}} + 2k_{\text{bf}} - 2(k_{\text{bf}} - k_{\text{p}})\phi}{k_{\text{p}} + 2k_{\text{bf}} - (k_{\text{bf}} - k_{\text{p}})\phi} \right] + 5 \times 10^4 \beta_1 \rho_{\text{bf}} c_{\text{bf}} f(T, \phi) \sqrt{\frac{K_{\text{B}} T}{\rho_{\text{bf}} d_{\text{p}}}} \quad (34)$$

where β_1 is the fraction of the liquid volume which travels with a particle and decreases with particle volumetric concentration because of the viscous effect of the moving particles. The values of β_1 for certain particles are given in Table 1. They introduced an empirical equation for $f(T, \phi)$ using the experimental data of Das et al. (2003) for CuO nanofluids valid in the range of $1 < \phi < 4 \%$ and $300 < T < 325 \text{ K}$ given by:

$$f(T, \phi) = (-6.04\phi + 0.4705)T + (1722.3\phi - 134.63)$$

In another paper, Koo and Kleinstreuer (2005) studied the influence of different motion mechanisms such as Brownian, thermophoresis, and osmophoresis on thermal conductivity of nanofluids. They reported the influence of Brownian motion to be significant on thermal conductivity ratio compared to thermophoresis and osmophoresis. The Brownian motion is influenced by particle size, whereas motion due to thermophoretic and osmophoretic effects is observed to be independent of particle size.

Table 1 Value of β_1 to be used with Eq. (34) of Koo and Kleinstreuer (2005)

Sl. No.	Type of particles	β_1	% Concentration/temperature range	Authors
1	Au citrate, Ag citrate, and CuO	$0.0137(100\phi)^{-0.8229}$	$\phi < 1$	Koo and Kleinstreuer (2005)
2	CuO	$0.0011(100\phi)^{-0.7272}$	$\phi > 1$	Koo and Kleinstreuer (2005)
3	Al ₂ O ₃	$0.0017(100\phi)^{-0.0841}$	$\phi > 1$	Koo and Kleinstreuer (2005)
4	Al ₂ O ₃	$8.4407(100\phi)^{-1.07304}$	$1 < \phi < 10\%$, $298 < T_{nf} < 363$ K	Vajjha and Das (2009)
5	ZnO	$8.4407(100\phi)^{-1.07304}$	$1 < \phi < 7\%$, $298 < T_{nf} < 363$ K	Vajjha and Das (2009)
6	CuO	$9.8810(100\phi)^{-0.9446}$	$1 < \phi < 6\%$, $298 < T_{nf} < 363$ K	Vajjha and Das (2009)

The combined Maxwell–Garnett conduction and convection caused by the Brownian motion of the suspended particles are the basis for thermal conductivity enhancement, according to Prasher et al. (2006). They proposed an equation for the estimation of thermal conductivity ratio based on the model given by:

$$\frac{k_{nf}}{k_{bf}} = (1 + 4 \times 10^4 Re_B^m Pr_{bf}^{0.33} \phi) \left[\frac{\{k_p(1 + 2\alpha) + 2k_m\} + 2\phi\{k_p(1 - \alpha) - k_m\}}{\{k_p(1 + 2\alpha) + 2k_m\} - \phi\{k_p(1 - \alpha) - k_m\}} \right] \tag{35}$$

where $m = 2.5$

$k_m = k_{bf}(1 + 0.25Re_B Pr)$ is the matrix conductivity

$Re_B = \frac{1}{\phi} \sqrt{\frac{18k_B T}{\pi \rho_p d_p}}$ is the Brownian–Reynolds number

$\alpha = \left(\frac{2R_b k_m}{d_p}\right)$ nanoparticle Biot number

R_b interfacial thermal resistance between nanoparticle and the surrounding fluid.

The authors ignored the interfacial resistance in their analysis and stated that it could be considered in the calculations using the model of Every et al. (1992). Leong et al. (2006) developed a model to determine the effective thermal conductivity of nanofluids taking into account the effect of interfacial layer at the particle/liquid interface.

$$k_{nf} = k_{bf} \frac{(K_p - k_i) \varnothing k_i [2\beta_2^3 - \beta^3 + 1] + (K_p + 2k_i) \beta_2^3 [\varnothing \beta^3 (k_i - K_{bf}) + K_i]}{\beta_2^3 (K_p + k_i) - (K_p - k_i) \varnothing [\beta_2^3 - \beta^2 - 1]} \quad (36)$$

where

$$\beta_2 = \left(1 + \frac{t}{a_p} \right)$$

According to Jang and Choi (2007), there are four mechanisms contributing to the energy transfer responsible for the enhancement of thermal conductivity of nanofluids. The first mode is collision between the base fluid molecules, the second is the thermal diffusion of nanoparticles, the third is the collision of nanoparticles with each other due to Brownian motion, and the fourth is collision between the base fluid molecules and nanoparticles due to thermally induced fluctuations. They developed an equation for the evaluation of the effective thermal conductivity of nanofluid given by:

$$k_{nf} = k_{bf}(1 + \varnothing) + \beta_3 k_p \varnothing + C_1 \frac{d_{bf}}{d_p} k_{bf} Re_d^2 Pr_{bf} \varnothing \quad (37)$$

where $\beta_3 = 0.01$, $C_1 = 18 \times 10^6$, $Re_d = \frac{C_{RM} d_p}{\eta}$, $C_{RM} = \frac{K_B T}{3\pi \mu_{bf} d_p l_{bf}}$ and is a constant considering the Kapitza resistance per unit area. The equivalent diameter $d_{bf} = 0.384, 0.561$ and mean free path, $l_{bf} = 738, 0.875$ nm, at 300 K are the values considered for water and EG-based nanofluids, respectively. The experimental data of Al_2O_3 and CuO in water and EG, Cu/EG are observed to be in good agreement with the values estimated with Eq. (37).

Murshed et al. (2008) solved the steady-state heat conduction equation considering interfacial layer with appropriate boundary conditions for cylindrical and spherical coordinate system. The numerical values are compared with the experimental data for spherical particles of Al_2O_3 (80 nm), TiO_2 (15 nm) in ethylene glycol, Al_2O_3 (38.4, 47, and 150 nm) in water, and CNT in engine oil. In another paper, Murshed et al. (2009) included the dynamic Brownian motion to the static conduction model in deriving an equation for effective thermal conductivity of nanofluid, which has the flexibility to be reduced to Maxwell’s equation in the absence of interaction between the nanoparticle and interfacial layer. The authors showed good agreement of theory with the experimental data of various investigators.

Khanafar and Vafai (2011) have given a few general correlations for the effective thermal conductivity of Al_2O_3 /water and CuO/water nanofluids at ambient temperatures accounting for various volume fractions and nanoparticle diameters. Equation (38) proposed using the experimental data of Al_2O_3 /water and CuO/water nanofluids, respectively, is given by:

$$k_{nf} = \left[1.0 + 1.0112\phi + 2.4375\phi \left(\frac{47}{d_p} \right) - 0.0248\phi_p \left(\frac{k_p}{0.613} \right) \right] k_{bf} \quad (38)$$

Equation (38) is applicable for ambient range of temperature.

$$k_{nf} = \left[0.9843 + 0.398\phi^{0.7383} \left(\frac{1}{d_p} \right)^{0.2246} \left(\frac{\mu_{nf}(T)}{\mu_f(T)} \right)^{0.0235} - 3.9517 \frac{\phi}{T} + 34.0.341 \frac{\phi}{T^2} \right] k_{bf} \quad (39)$$

where $\mu_f(T) = 2.414 \times 10^{-5} \times 10^{-247.8(T-140)}$ and valid for $11 \leq d_p \leq 150$ nm; $20^\circ \text{C} \leq T \leq 70^\circ \text{C}$.

Thus, the theoretical models developed till now are improvement of Maxwell's equation with the consideration of (i) shells/interface on the surface of the particle (ii) Brownian motion (iii) interaction between base liquid molecules or nanoparticles and (iv) base liquid molecules and nanoparticles. Certain models include parameters such as mean free path of water used in the process of obtaining dimensionless terms.

3.2 Experimental Thermal Conductivity, k_{nf}

It can be observed that most of the investigators who improved Maxwell's models used certain empiricism in their equations. Early determination of nanofluid thermal conductivity through experiments was undertaken using base liquid as water.

Pak and Cho (1998) determined the thermal conductivity of Al_2O_3 and TiO_2 nanofluids at 27°C which can be presented as:

$$k_{nf} = (1 + 7.47\phi)k_{bf} \quad (40)$$

The determination of nanofluid thermal conductivity based on experiments has grown rapidly since the work of Lee et al. (1999) who conducted experiments with Al_2O_3 and CuO nanoparticles of sizes 38 and 24 nm, respectively, in water and EG using transient hot-wire method. The experimental data with $\text{Al}_2\text{O}_3/\text{water}$ and $\text{Al}_2\text{O}_3/\text{EG}$ are observed to be in close agreement, whereas CuO/water and CuO/EG nanofluids showed higher values when compared with Hamilton–Crosser model. They reasoned that the obtained lower values of thermal conductivity with $\text{Al}_2\text{O}_3/\text{water}$ were due to larger particle size of 38 nm used when compared with the values of Masuda et al. (1993) who used 13-nm-sized particles. They opined that the equation of Hamilton–Crosser is capable of predicting thermal conductivity of large agglomerated clusters but inadequate for nanosized particles. Xuan and Li (2000) reported the thermal conductivity ratio of Cu/water to increase between 1.24 and

1.78 for corresponding volume concentration of 2.5–7.5 %. The particle size is reported to be lower than 100 nm; the average size was not disclosed.

Yu et al. (2000) reported the observation of molecular layering at the solid–liquid interface from X-ray reflectivity data. Spherical Tetrakis (2-ethylhexoxy) silane (TEHOS) liquid molecules of size 10 Å diameter are used in the experiment. Silicon substrates of 45–90 Å thick are prepared, and reflectively measurements were undertaken. They reported the measurement of oscillations near the solid–liquid interface with a period of about 10 Å, common to all samples and independent of the film thickness.

Xie et al. (2002) obtained a maximum enhancement of 15.8 % in thermal conductivity with 26-nm spherical SiC/water nanoparticles at a volume concentration of 4.2 %. The thermal conductivity is reported to increase linearly with concentration in the lower range.

Das et al. (2003) determined the thermal conductivity of 29 nm CuO/water and 38 nm Al₂O₃/water. They reasoned the deviation of 24 nm CuO/EG and CuO/water experimental data of Lee et al. (1999) to the ‘insensitive’ nature of Hamilton and Crosser Eq. (27) for temperature.

Murshed et al. (2005) reported 30 % enhancement in thermal conductivity of water-based TiO₂ nanofluid with particle size of 15 nm at 5 % vol concentration. Zhu et al. (2006) measured the thermal conductivity of Fe₃O₄ nanofluid in base liquid water. They observed a nonlinear variation of thermal conductivity ratio with volume fraction from their experimental data and reported relatively higher enhancement rate at lower volume fractions.

Li and Peterson (2006) undertook experimental investigations to determine the influence of thermal conductivity on volume concentration and temperature. The experiments are conducted with sizes of 29 nm of CuO/water and 36 nm of Al₂O₃/water, temperatures ranging from 27.5 to 34.7 °C for 2–10 % volume fractions. A linear regression equation for the estimation of thermal conductivity ratio based on temperature and volume fraction is presented for Al₂O₃ and CuO nanofluids, respectively, as:

$$k_{nf}/k_w = (0.69266 + 3.761088\phi + 0.4705T) \tag{41}$$

$$k_{nf}/k_w = (0.53785 + 0.7644815\phi + 0.018689) \tag{42}$$

The values of thermal conductivity obtained by Li and Peterson (2006) reported monotonic decrease in thermal conductivity with increasing particle size. The results indicate the dependence of effective thermal conductivity on material suspensions, particle size, concentration/volume fraction, and the bulk temperature.

Yoo et al. (2007) measured the thermal conductivities of TiO₂ (25 nm) and Al₂O₃ (48 nm) dispersed in deionized water and Fe (10 nm) and tungsten trioxide WO₃ (38 nm) dispersed in EG and reported high enhancements with Fe and WO₃ nanofluids. Hwang et al. (2007) determined the thermal conductivity of MWCNT, fullerene, CuO, and SiO₂ in deionized water, EG, and oil. The thermal conductivity

of nanofluid increased with concentration except for water-based fullerene ($k_p = 0.4 \text{ W/mK}$) which is lower than water.

Experiments have been conducted by Mintsa et al. (2009) to estimate the thermal conductivity of aluminium oxide (36 and 47 nm) and copper oxide (29 nm) nanofluids in water in the temperature range of 20–50 °C and up to 18 % volume concentration. Linear equations with volume concentration applicable at ambient temperature for these nanofluids are given, respectively, as:

$$k_{nf}/k_w = 1.0 + 1.72\phi \quad (43)$$

$$k_{nf}/k_w = 0.99 + 1.74\phi \quad (44)$$

It can be observed that the values of the oxide nanofluids estimated with Eqs. (43) and (44) at different volume concentrations do not vary significantly for the two materials. The thermal conductivity data obtained at higher temperatures and volume concentration are observed to be in good agreement with the Eq. (33) of Chon et al. (2005).

Garg et al. (2008) have investigated the thermal conductivity of Cu (200 nm) nanoparticles in ethylene glycol in the concentration range of 0.5–2.5 %. Based on their experimental thermal conductivity data, a linear equation is presented as:

$$k_{nf} = (1 + 6\phi)k_{br} \quad (45)$$

Mintsa et al. (2009) observed that Eq. (33) given by Chon et al. (2005) is in good agreement with the experimental data of both $\text{Al}_2\text{O}_3/\text{water}$ and CuO/water nanofluids. Sundar et al. (2013) determined the effective thermal conductivity of magnetic $\text{Fe}_3\text{O}_4/\text{water}$ nanofluid experimentally in the volume concentration range of 0–2.0 % in the temperature range of 20–60 °C. Thermal conductivity enhancement at the temperatures of 20 and 60 °C is reported to be, respectively, 8.4 and 17 % at $\phi = 0.2\%$ and 25 and 48 % at $\phi = 2.0\%$ concentration.

3.3 k_{nf} in Base Liquid Ethylene Glycol

Lee et al. (1999) investigated oxide nanofluids by suspending CuO 35-nm particles in ethylene glycol. A 20 % increase in thermal conductivity at 4 % volume is reported by them. Eastman et al. (2001) determined the thermal conductivity of Cu/EG nanofluid. They observed a maximum enhancement of 40 % in thermal conductivity at 0.3 % volume concentration with 10-nm-sized particles dispersed in ethylene glycol. The enhancement with CuO/EG and $\text{Al}_2\text{O}_3/\text{EG}$ of 35-nm-sized particles at a volume concentration of 4 % is approximately 20 %.

Wang et al. (2002) determined the thermal conductivity of Al_2O_3 , ZnO, TiO_2 , CuO, Fe_2O_3 , Cerium oxide (CeO_2) nanoparticles in base liquid ethylene glycol for 0.5, 1.5, 3.0 and 4.0 % concentration at an ambient temperature of 25 °C. The

maximum thermal conductivity enhancement was observed at 4 % volume concentration varied between 13 and 21 % for the nanofluids considered.

Xie et al. (2010) undertook thermal conductivity determination with MgO, TiO₂, ZnO, Al₂O₃, and SiO₂ nanoparticles dispersed in base liquid EG. They observed MgO/EG nanofluid to have superior features of the highest thermal conductivity and the lowest viscosity when compared with other nanofluids. The enhancement of 40.6 % is reported with MgO nanofluid at 30 °C for a volume concentration of 5 %.

Murshed (2011) determined the thermal conductivity of nanofluids which are prepared by suspending TiO₂ (15 nm), Al₂O₃ (80 nm), and Al (80 nm) nanoparticles in ethylene glycol for a maximum concentration of 5 %. The TiO₂ nanofluid at 5 % concentration, a maximum enhancement of thermal conductivity is reported to be 17 %. However, the enhancement in thermal conductivity at the same concentration of 5 % with Al and Al₂O₃ is observed to be 45 and 14 %, respectively.

3.4 k_{nf} in Ethylene Glycol Water Mixtures

Sun and Teja (2004) determined the thermal conductivity, viscosity, and density for different ratios of EG/water mixture and presented linear equations for their estimation. Kim et al. (2007) estimated the thermal conductivity of Al₂O₃, ZnO, and TiO₂ nanofluids in water and ethylene glycol. They reported linear increase in thermal conductivity with nanofluid concentration. The enhancement is observed to increase with the decrease in particle size for the two base fluids undertaken.

Karthikeyan et al. (2008) determined the thermal conductivity of CuO (8 nm) nanofluid in base liquid water and ethylene glycol for 1.0 % volume concentration. They observed enhancements of 31 and 54 % with CuO/water and CuO/EG, respectively, and the temperature of the nanofluid was not specified. Patel et al. (2010) observed enhancement of 11.5 and 14 % with CuO/water and CuO/EG at 50 °C with a particle size of 31 nm. The significant enhancement in thermal conductivity is attributed to the finer particle size and monodispersion of nanoparticles in the base liquid. It has been observed that the thermal conductivity of nanofluid increases nonlinearly with the volume fraction of nanoparticles.

Vajjha and Das (2009) measured the thermal conductivities of Al₂O₃, CuO, and ZnO nanofluids with particles dispersed in EG/water mixture in the ratio of 60:40 by mass. They conducted experiments in the temperature range of 25–90 °C for volume concentration up to 10 % and observed the data to fit in Eq. (34) of Koo and Kleinstreuer (2005) resulting in obtaining new relations for $f(T, \phi)$ and β_1 given by:

$$f(T, \phi) = (2.8217 \times 10^{-2} \phi + 3.917 \times 10^{-3}) \left(\frac{T}{T_o} \right) + (-3.0669 \times 10^{-2} \phi - 3.91123 \times 10^{-3}) \quad (46)$$

The relations for β_1 are listed in Table 1 for different nanofluids.

Beck et al. (2010) determined the thermal conductivity of Al_2O_3 nanofluids in water, EG, and 50:50 ratio of EG/water mixture. They undertook experiments with Al_2O_3 of 10 and 50 nm particle sizes in EG/water mixture and 12 nm in both water and EG base liquids to determine the thermal conductivity at different temperatures and concentrations up to a maximum of 4.93 % by volume. They attributed a decrease in nanofluid thermal conductivity due to changes in phonon transport as the particle size increases from 10 to 50 nm.

Yu et al. (2012) investigated the heat transfer properties of Al_2O_3 experimentally using a mixture of ethylene glycol and water in the ratio of 45:55 by volume and observed thermal conductivity enhancement of 3.8 and 11.8 % for volume concentrations of 1 and 3 %, respectively. They observed Al_2O_3 nanofluid to exhibit Newtonian and non-Newtonian behaviour for temperatures greater than 45 °C and below 45 °C, respectively, at 2.0 % volume concentration.

Sahoo et al. (2012) conducted experimental investigations for the determination of thermal conductivity of SiO_2 (20 nm) nanoparticles dispersed in 60:40 EG/water by mass, in the temperature range of 20–90 °C for a maximum concentration of 10 vol%. An enhancement of 20 % in thermal conductivity was reported at $\phi = 10\%$ and 87 °C. An equation for the estimation of thermal conductivity at 6 % concentration of nanofluid valid in the temperature range of 290–365 K is given by:

$$k_{\text{nf}} = \left[-0.45577 \left(\frac{T}{T_o} \right)^2 + 1.72837 \left(\frac{T}{T_o} \right) - 0.18589 \right] k_{\text{bf}}; \quad T_o = 293 \text{ K} \quad (47)$$

Branson et al. (2013) prepared nanofluid by deaggregation of diamond oxide in dimethyl sulphoxide followed by reaction with glycidol monomer, purification via aqueous dialysis, and dispersion in EG base fluid. It is observed that diamond (11 nm) nanofluid exhibited 12 % enhancement in thermal conductivity at 0.9 % vol concentration. In a similar manner when diamond oxide is deaggregated in the presence of oleic acid followed by dispersion in a light mineral oil, the oil-based dispersions of nanodiamond (ND) exhibited 11 % enhancement in thermal conductivity with a particle size of 18 nm at 1.9 % vol concentration. From the experimental values, equations for the estimation of thermal conductivity are presented which are given by:

$$k_{\text{nf}} = (1 + 14\phi)k_{\text{bf}}; \text{ ND} - \text{EG} \quad (48)$$

$$k_{\text{nf}} = (1 + 6\phi)k_{\text{bf}}; \text{ ND} - \text{MO} \quad (49)$$

Sundar et al. (2014) prepared nanofluids by dispersing Al_2O_3 particles in EG–water mixture ratio of 20:80, 40:60, and 60:40 by weight. The thermal conductivity and viscosity are determined between 20 and 60 °C in the volume concentration range of 0.3–1.5 %. A maximum thermal conductivity enhancement of 32.26 %

was reported with 20:80 % EG/water nanofluid at 1.5 % volume concentration at a temperature of 60 °C.

3.5 *Effect of PH on Nanofluid Thermal Conductivity*

Murshed et al. (2005) conducted experiments with TiO₂ (15 nm) nanofluid with cetyltrimethylammonium bromide (CTAB) surfactant to ensure uniform dispersion of spherical particles in base liquid water. The pH of the nanofluid is maintained between 6.8 and 6.2 for particle volume concentrations between 0.1 and 2.0 %. The enhancement is 17 % greater than the values predicted by Hamilton–Crosser and Bruggeman models at 5 % nanofluid concentration, while the temperature of the nanofluid is not disclosed.

Yurong He et al. (2007) maintained a pH value of 11 in the absence of stabilizer by dispersing TiO₂ (20 nm) nanoparticles in water. The values of thermal conductivity from their experiments are reported to be lower than those obtained by Murshed et al. (2005). The difference in the thermal conductivity value is attributed to a large difference in pH value employed in addition to larger particle size used by Yurong He et al. (2007). This is in conformity with the observations of Xie et al. (2002) who observed thermal conductivity to increase with the decrease in pH (from basic to acidic range).

Li et al. (2008) optimized the use of sodium dodecylbenzene sulphonate (SDBS) surfactant for Cu/water (25 nm) suspensions to maintain pH in the range of 8.5–9.5 for enhanced thermal conductivity. The maximum thermal conductivity enhancement of 10.7 % is observed with 0.10 wt% suspension. Wang et al. (2009) conducted experiments to determine the thermal conductivity of Al₂O₃/water and Cu/water-based nanofluids for 0.02, 0.05, 0.1, and 0.15 % weight concentrations at different pH values by adding different quantities of SDBS. They observed a maximum thermal conductivity enhancement of 7, 8, 8.5, and 10 % for Al₂O₃/water and 8, 9, 11, and 12 % for Cu/water when the pH is maintained at 7.5 and 9.0 for Al₂O₃/water and Cu/water, respectively.

3.6 *Effect of Particle Size on k_{nf}*

Xie et al. (2001) prepared non-oxide ceramic (SiC) nanofluid with particle size varying between 26 and 600 nm. Xie et al. (2002) produced Al₂O₃ nanofluid with particle size ranging from 1.2 to 302 nm to determine the influence of particle size on thermal conductivity.

Kim et al. (2007) measured thermal conductivity of alumina, ZnO (10, 30, and 60 nm), and TiO₂ (10, 35, and 70 nm) particle suspensions in water and ethylene glycol up to 3.0 % volume concentration. They determined a maximum thermal conductivity enhancement with ZnO/water nanofluid of 14.2, 11.5, and 7.3 % with

10-, 30-, and 60-nm-sized particles, respectively, at 3 % concentration. At the same concentration, the value of maximum thermal conductivity enhancement for ZnO/EG is reported to be 21 and 10.7 % with 30- and 60-nm-sized particles, respectively. The maximum enhancement values for TiO₂ (10, 35, and 70 nm)/water are 11.4, 8.7, and 6.4 %, and for TiO₂ (10, 35, and 70 nm)/EG, the values are 15.4, 12.3, and 7.5 %, respectively.

Chon et al. (2005) observed 4.8–15.8 % enhancement in nanofluid thermal conductivity k_{nf} when the size of Al₂O₃ nanoparticles in water decreased from 150 to 11 nm. Similar observations have been reported by other researchers like Mintsa et al. (2009), He et al. (2007) including the recent study of Kazemi-Beydokhti et al. (2014) who has determined thermal conductivity with Al (25 nm), Al₂O₃ (30 nm), CuO (18 nm), SnO₂ (20 nm), SiO₂ (12 nm) and TiO₂ (35 nm) water-based nanofluids in the temperature range of 20–60 °C.

An increase in thermal conductivity of magnetite (Fe₃O₄) nanoparticles with particle size of less than 10 nm has been observed by Shima et al. (2009). The Fe₃O₄ nanoparticles have been prepared in the range of 2.8–9.5 nm by precipitating iron salts with sodium hydroxide using an established procedure and stabilized with a protective surfactant layer. Nanofluid thermal conductivity at 1.0 and 5.5 % volume concentrations, at 25 °C, in an oil-based carrier fluid has been estimated. They observed an increase in nanofluid thermal conductivity with particle size and attributed the thermal conductivity enhancement to the agglomeration of nanoparticles. The observation of Shima et al. (2009) for particle size lower than 10 nm is contrary to the observed phenomenon with particle size larger than 10 nm by Jang and Choi (2004) and Feng et al. (2008).

Beck et al. (2010) conducted experiments with Al₂O₃ nanoparticles in water and ethylene glycol at five different sizes in the range of 8–282 nm. They concluded from their experimental analysis that the rate of thermal conductivity enhancement is significant for particle size below 50 nm with no significant change thereafter.

Teng et al. (2010) studied the effect of particle size, temperature, and concentration on the thermal conductivity ratio of Al₂O₃ (20, 50, and 100 nm) nanofluid dispersed in water in the concentration range of 0.5–2.0 % and temperature range of 10–50 °C. The enhancement in thermal conductivity is reported to be 6.5, 6.0, and 5.6 % measured at 10 °C and 14.7, 7.3, and 5.6 % at 50 °C for the particle sizes of 20, 50, and 100 nm, respectively. They observed a decrease in thermal conductivity of Al₂O₃ with the increase in particle size measured at temperatures of 10 and 50 °C.

Patel et al. (2010) have presented thermal conductivity experimental data for oxide and metal nanofluids for different particle–base fluid combinations, particle size, volume fraction and temperature using transient hot wire and temperature oscillation equipment. The experiments are undertaken with Cu (80 nm), CuO (31 nm), and Al₂O₃ (11, 45, and 150 nm) nanofluids in the concentration range of $0 < \phi < 3\%$ and temperature between 20 and 50 °C. The maximum enhancement in thermal conductivity was observed to be 38 and 26 % with Cu and CuO nanofluids, respectively, in transformer oil at 9.27 and 9.11 % volume concentration at 50 °C, respectively. The maximum enhancement reported is 32 and 18 % with Al₂O₃ (11 nm) suspended in EG and water, respectively, at 50 °C with 3 %

volume concentration. A nonlinear regression analysis is undertaken for the thermal conductivity estimation of spherical shaped oxide and metal nanofluids given by:

$$k_{nf} = \left[1.0 + 0.135 \left(\frac{k_b}{k_p} \right)^{0.273} \phi^{0.467} \left(\frac{T}{20} \right)^{0.547} \left(\frac{100}{d_p} \right)^{0.234} \right] k_{bf} \quad (50)$$

An empirical correlation is proposed by Corcione (2011) for the determination of nanofluid thermal conductivity. The experimental data of alumina, copper oxide, titania, and copper nanoparticles determined by various investigators with particle diameters in the range of 10–150 nm and suspended in water and EG are used in their analysis. An Eq. (51) with a mean deviation of 1.86 % is presented.

$$\frac{k_{nf}}{k_{bf}} = 1 + 4.4Re^{0.4}Pr_{bf}^{0.66} \left[\frac{T}{T_{fr}} \right]^{10} \left[\frac{k_p}{k_{bf}} \right]^{0.03} \phi^{0.66} \quad (51)$$

where $Re = \frac{2\rho_{bf}k_{bf}T}{\pi\mu_{bf}^2d_p}$ is the nanoparticle Reynolds number, Pr_{bf} is the Prandtl number of the base liquid, T is the nanofluid temperature, T_{fr} is the freezing point of the base liquid, and k_p is the nanoparticle thermal conductivity. The equation is applicable for volume concentrations up to 9 % in the temperature range of 294–324 K.

The investigators observed the thermal conductivity ratio to depend on the material, particle size, volume concentration, and nanofluid temperature in their study. It can be concluded that nanofluid thermal conductivity increases with a decrease in particle size. A few other studies suggest the dependence of particle size on thermophysical properties which can influence the thermal conductivity of nanofluids.

3.7 Effect of Size on Particle Specific Heat

The influence of particle size on thermal conductivity is supported with the theoretical and experimental observations by Wang et al. (2006) who studied the effect of particle size on specific heat capacity. The values of bulk specific heat obtained with CuO nanoparticles from experiments are found to be in close agreement with the theoretical predictions for temperatures lower than 225 K for particles up to 50 nm. However, for temperatures above 225 K, the theoretical values of specific heat capacity decrease as the particle size is reduced from 50 to 10 nm. For particles below 10 nm, the specific heat capacity increases with particle size.

Wang et al. (2006) reasoned that for particles larger than 10 nm, the quantum effect can be neglected and the specific heat will decrease monotonically as the particle size is reduced from 50 to 10 nm. For particles that are smaller than 10 nm, the quantum effect will increase the specific heat capacity of the nanoparticles

uniformly and thus create an irregular behaviour for particles of different sizes. This observation is also stated to be in conformity with the monotonic decreasing relation proposed by Prasher et al. (2006).

The experimental observations indicate the dependence of material, concentration, particle size, temperature, and the influence of pH value on nanofluid thermal conductivity. The following observations can be made from the investigations undertaken:

- The thermal conductivity of metal and oxide nanofluids is observed to be greater than that of equivalent macroparticle suspensions.
- Experiments for the determination of nanofluid thermal conductivity are undertaken mostly with spherical particles having diameters in the range of 20–300 nm and temperature between 20 and 70 °C having Newtonian properties for a maximum volume concentration of 4.0 % in base liquid water, EG, and EG/water mixtures.
- Experimental data have confirmed higher thermal conductivities than the base liquid which increases with concentration and temperature.
- The conductivity ratios of ethylene glycol-based nanofluids are reported to be higher than those of water-based nanofluids.
- Metal nanofluids have higher enhancements than those of oxide nanofluids.
- Nanofluid thermal conductivity is relatively higher at lower volume fractions, thereby giving a nonlinear dependence on particle volume fraction.
- The experimental results indicate the thermal conductivity ratio to increase linearly with volume fraction, but with different rates of increase for each nanofluid.
- Nanofluid thermal conductivity is observed to depend on particle size and suspension temperature.
- Material properties influence the thermal conductivity of nanofluids leading to higher enhancements compared to viscosity. This observation may vary with temperature, nanofluid concentration, and particle size.

It can be observed from Eqs. (25)–(50) that particle thermal conductivity k_p is considered in the development of equations for the estimation of nanofluid thermal conductivity k_{nf} . The equations developed do not consider the impact of material density and specific heat on nanofluid thermal conductivity. Since the properties are different, their influence on nanofluid thermal conductivity k_{nf} can be included with thermal diffusivity term α_p . Hence, the experimental data of water-based nanofluids are used in the development of a regression equation by Sharma et al. (2010) as:

$$k_r = \frac{k_{nf}}{k_w} = \left[0.8938 \left(1 + \frac{\phi}{100} \right)^{1.37} \left(1 + \frac{T_{nf}}{70} \right)^{0.2777} \left(1 + \frac{d_p}{150} \right)^{-0.0336} \left(\frac{\alpha_p}{\alpha_w} \right)^{0.01737} \right] \quad (52)$$

The correlation equation is validated with 252 data values with a maximum deviation of 11 % for a few points. The experiments are conducted mostly with spherical shaped particles having diameters in the range of 20–150 nm, temperatures between 20 and 70 °C, and a volume concentration of less than 4.0 %.

4 Nanofluid Specific Heat

According to Wang et al. (2006), specific heat capacity of a particle varies with particle size. Since smaller particles have larger specific surface areas, the influence of surface energy on the effective specific heat capacity increases with a reduction in particle size. Ping Zhou et al. (2010) showed the deviation of specific heat capacity of CuO/EG nanofluid at different volume concentrations evaluated using equations given by Eqs. (53) and (54) with their experimental data.

$$C_{\text{pnf}} = \frac{(1 - \phi)(\rho C_p)_{\text{bf}} + \phi(\rho C_p)_p}{(1 - \phi)\rho_{\text{bf}} + \phi\rho_p} \tag{53}$$

$$C_{\text{pnf}} = \phi C_p + (1 - \phi)C_{\text{bf}} \tag{54}$$

It can be observed from their results that experimental values of specific heat capacity decreased from 2550 to 2450 kJ/(kg K) with the increase in volume concentration between 0.1 and 0.6 %. The experimental values are higher than the values calculated with Eqs. (53) and (54) which are based on the law of mixtures. However, the variation of heat capacities with volume concentration is observed to be constant. Ping Zhou et al. (2010) state that the deviation in the values of heat capacity of nanofluids for different sizes of nanoparticles is not significant with increasing volume concentration, due to the large specific heat capacity of the base fluid. Based on the observations of Wang et al. (2006) and Zhou et al. (2010), it can be concluded that the heat capacity of particle varies, while that of nanofluid remains constant with the size of the nanoparticle.

Zhou and Ni (2008) measured the specific heat of Al₂O₃/water nanofluids using a differential scanning calorimeter, with Al₂O₃ particle size of 45 nm at a temperature of 33 °C in the concentration range of 00–21.7 vol%. The specific heat of Al₂O₃, ZnO₂, and SiO₂ nanoparticles has been determined by Vajjha and Das (2009). The first two nanoparticles are dispersed in the base fluid mixture of ethylene glycol and water (60:40 EG/W) and the third silicon dioxide in deionized water. The samples of Al₂O₃, ZnO, and SiO₂ nanofluids tested had average particle sizes of 44, 77, and 20 nm, respectively. Measurements were undertaken over a temperature range of 315–363 K. The nanoparticle volumetric concentrations tested were up to 10 %. The equation that best fits the experimental data of all three nanofluids prepared from two kinds of base fluids is given as:

$$C_{p,\text{eff}} = \left[\frac{(A \times T) + \left(\frac{C_{p,p}}{C_{p,\text{bf}}}\right)}{C + \emptyset} \right] C_{p,\text{bf}} \quad (55)$$

$$\text{Al}_2\text{O}_3 : A = 0.0008911; B = 0.5719; C = 0.4250$$

$$\text{SiO}_2 : A = 0.001769; B = 1.1937; C = 0.8021$$

$$\text{ZnO} : A = 0.0004604; B = 0.9855; C = 0.2990$$

Murshed et al. (2011) observed that nanofluids at low concentrations have lower values of effective specific heat than their base fluids. Barbés et al. (2013) have measured the thermal conductivities and specific heat capacities of Al_2O_3 (40–50 nm) dispersed in water and ethylene glycol for a particle volume concentration of 1.0–10.0 % in the temperature range of 298 and 338 K. Yiamsawasd et al. (2012) determined the specific heat of TiO_2 and Al_2O_3 nanofluids in water and a mixture of EG/water (20/80 wt%). The measurement is based on a differential thermal analysis technique for a maximum concentration of 8.0 vol% and temperatures between 15 and 65 °C. The authors presented a correlation equation to predict the specific heat of Al_2O_3 and TiO_2 nanofluids in a form of specific heat ratio between nanofluids and base fluid given by:

$$C_{p,\text{eff}} = \left[A \emptyset^B T^C \left(\frac{C_{p,p}}{C_{p,\text{bf}}} \right) \right]^D C_{p,\text{bf}} \quad (56)$$

$$\text{Al}_2\text{O}_3 : A = 1.249458; B = -0.05846; C = 0.006467; D = -0.17236$$

$$\text{Al}_2\text{O}_3 : A = 1.387402; B = -0.06425; C = 0.001124; D = -0.21159$$

Sekhar and Sharma (2015) have conducted experiments to determine the specific heat of water-based nanofluids containing Al_2O_3 (47 nm) nanoparticles for 0.01–1.0 % concentration in the temperature range of 25–45 °C. They presented an equation for the determination of specific heat applicable for water-based nanofluids given by:

$$C_{p,\text{eff}} = \left[0.8429 \left(1 + \frac{T_{\text{nf}}}{50} \right)^{-0.3037} \left(1 + \frac{d_p}{50} \right)^{0.4167} \left(1 + \frac{\emptyset}{100} \right)^{2.272} \right] \quad (57)$$

The following observations can be made from the investigations undertaken on nanofluid specific heat:

- The nanofluid specific heat is lower than the values of base liquid.
- The specific heat of nanofluid decreases with the increase in concentration.
- The specific heat of nanofluid does not vary significantly with temperature.
- The deviation in the values of heat capacity of nanofluids for different sizes of nanoparticles is insignificant with increasing volume concentration, due to the

large heat capacity of the base fluid. Hence, the variation of heat capacity with volume concentration is a constant.

5 Density

The experimental determination of nanofluid density reported in the literature is limited compared to thermal conductivity and viscosity. Density measurements were performed by Vajjha et al. (2009) on three different nanofluids containing Al_2O_3 (44 nm), antimony tin oxide, $\text{Sb}_2\text{O}_5\text{:SnO}_2$ (22–44 nm), and ZnO (70 nm) nanoparticles in a base fluid of 60:40 EG/water by mass over a temperature range of 0–50 °C for concentration range of 1–10 %. A good agreement is observed between the measured values with Eq. (58) of Pak and Cho 1998 (1998) at all temperatures and concentrations for Al_2O_3 and $\text{Sb}_2\text{O}_5\text{:SnO}_2$ with maximum deviation of 1.2 %. However, a maximum deviation of 8.0 % is observed with ZnO nanofluid.

$$\rho_{\text{nf}} = \phi_p \rho_p + (1 - \phi) \rho_{\text{bf}} \tag{58}$$

Teng and Hung (2014) in their study analysed the density of Al_2O_3 /water nanofluid in the concentration range of 0–1.5 %. It is observed that by comparing the calculated values of density based on Eq. (58) with the experimental data, the deviation of density is observed to be in the range of –1.50 to 0.06 %. The calculated results of density show a trend of greater deviation as the concentration of nanofluid increases.

Mahian et al. (2013) have conducted experiments with ZnO (20 nm) nanoparticles suspended in EG/water mixture of weight ratio 40:60 in the temperature range of 25–40 °C for a maximum concentration of 4.0 %. The deviation in the values of nanofluid density with the values estimated with Eq. (58) is approximately 7.0 % at all volume fractions. The maximum density is observed to be 1328.72 kg/m³ at 25 °C for 4.0 vol%. Mariano et al. (2013) conducted experiments with SnO_2 (≈17 nm) dispersed in EG in the temperature range of 10–50 °C and between 1 and 5 % volume concentration. The maximum density was observed at 10.5 °C for 5.0 vol%. The following observations can be made from the investigations undertaken on nanofluid density:

- The nanofluid density is higher than that of the base liquid.
- The nanofluid density increases with concentration.
- The density of nanofluid decreases with the increase in temperature.

6 Results and Discussion

The variation of experimental data of viscosity with temperature reported by various investigators for TiO₂/water nanofluid is shown in Fig. 2 for particle diameter of 21 nm in the concentration range of 1.0–3.0 % volume. The variation of viscosity of SiO₂/EG water mixture with temperature is shown in Fig. 3 for different concentrations and particle size by Namburu et al. (2007) and Kulkarni et al. (2008). It can be observed from Figs. 2 and 3 that the viscosity increases with concentration and decreases with temperature for any base liquid. Further, from Fig. 2, the values of SiO₂/EG water mixture at 4.0 % concentration between researchers differ for the same particle size. However, the deviation of experimental

Fig. 2 Variation in experimental values of viscosity with temperature for TiO₂ nanofluid

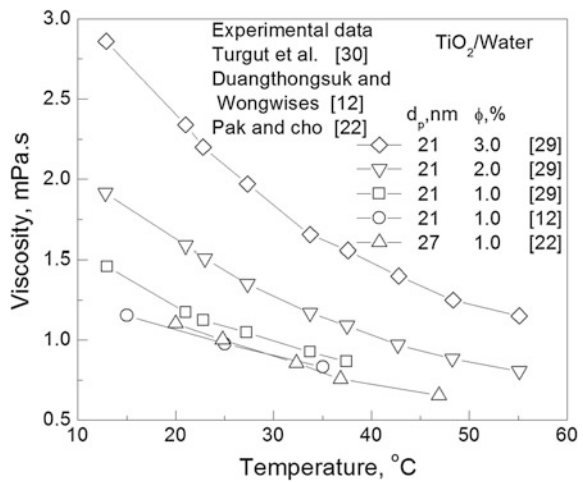
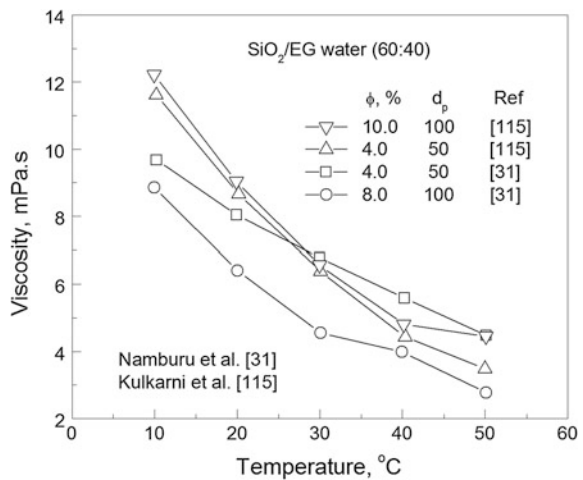


Fig. 3 Variation in experimental values of viscosity with temperature for different nanofluid concentrations and particle sizes



data for $\text{TiO}_2/\text{water}$ at 1.0 % concentration between the authors is about 30 % at lower temperature and decreases to about 20 % as the temperature increases. Consequently, the data of Duangthongsuk and Wongwises (2009) for viscosity of TiO_2 (21 nm)/water with concentration deviate from the lines drawn with Eqs. (53) and (54) shown in Fig. 4 by a maximum of 7.0 % due to different values reported by various researchers. This may be due to different methods of preparation employed, particle size dispersion, and pH among other factors resulting in the variation of viscosity.

The variation of thermal conductivity with concentration is shown in Figs. 5 and 6 for various nanofluids and particle size. It can be observed that the thermal conductivity increases with concentration. Metals show higher enhancements in comparison with oxide nanofluids. From the experimental data reported by various

Fig. 4 Comparison of experimental values of viscosity with equations for TiO_2 nanofluid

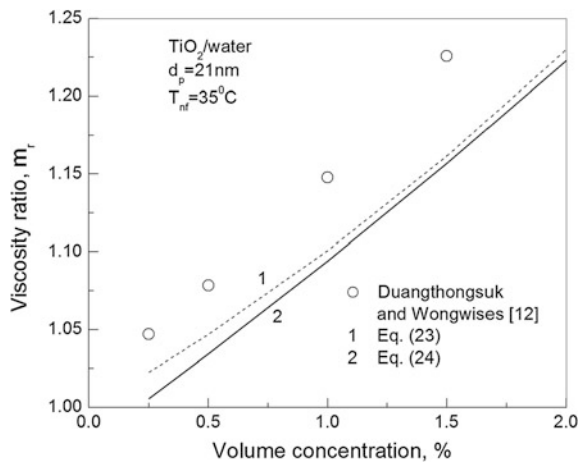
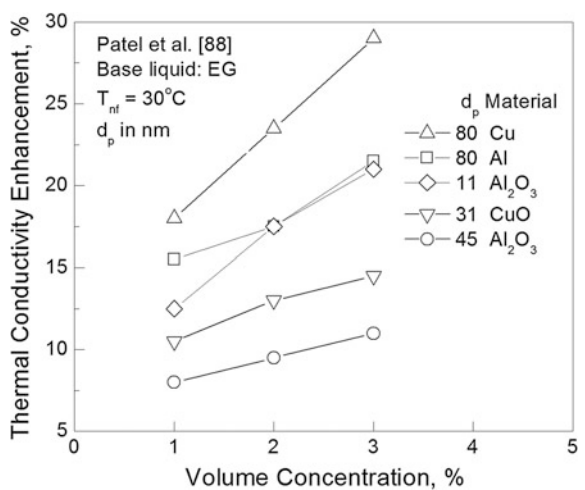


Fig. 5 Influence of nanofluid on thermal conductivity enhancement



investigators, it is possible that the thermal conductivity might reflect nonlinearity for concentrations lower than 1.0 % volume.

It can be observed from Fig. 6 that the enhancement with Al metal is greater with a particle size of 80 nm in comparison with its oxide having smaller particle size. The influence of particle size on thermal conductivity is shown in Fig. 7 with the experimental data of Beck et al. (2009), Kim et al. (2007). Most of the investigators observed a decrease in thermal conductivity with the increase in particle size. This is in agreement with the data of Kim et al. (2007) with TiO₂ and ZnO which reflect a decrease in thermal conductivity in contrast to the data of Beck et al. (2009).

The experimental data of nanofluid specific heat in different base liquids are shown in Fig. 8. The specific heat increases with temperature, and the enhancement

Fig. 6 Comparison of experimental data with various equations for thermal conductivity ratio

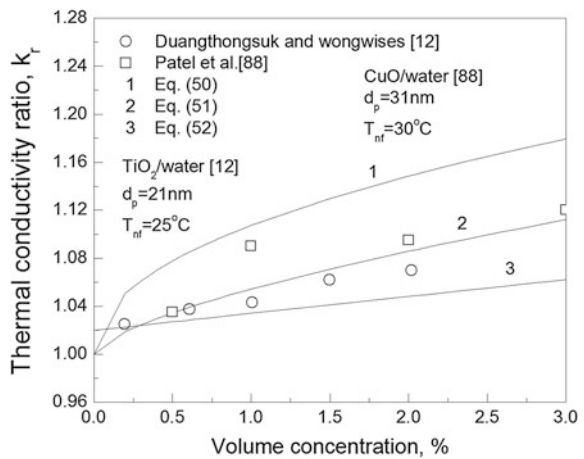


Fig. 7 Variation in experimental values of thermal conductivity with particle diameter for various metal oxides at 3 % volume concentration

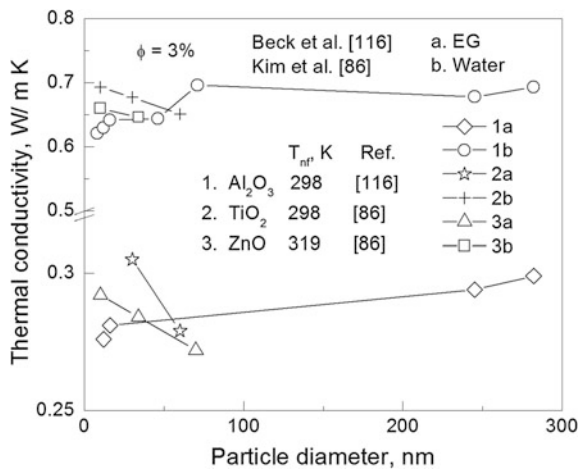


Fig. 8 Variation in experimental values of specific heat with temperature for different nanofluids in base liquid EG/water

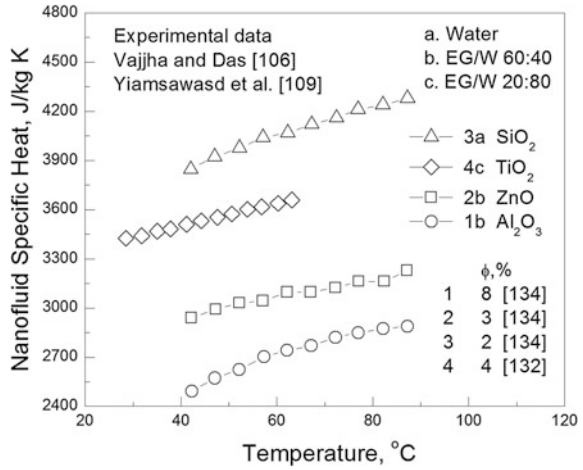
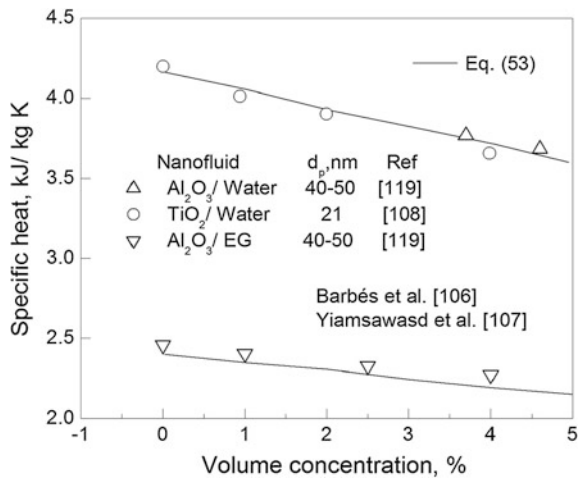


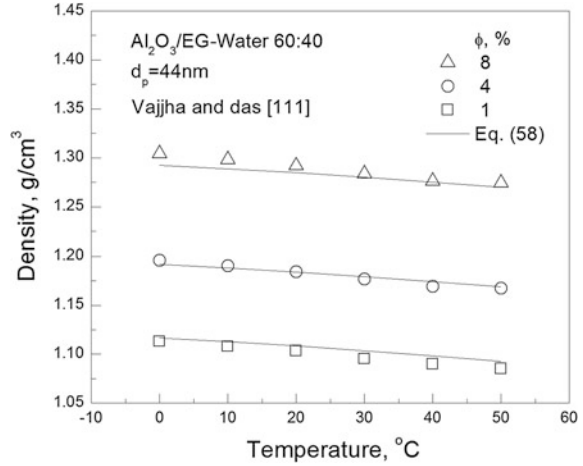
Fig. 9 Comparison of experimental data with mixture equation of specific



is pronounced for higher concentrations of nanofluid. The effect of concentration on nanofluid specific heat is shown in Fig. 9. The values of nanofluid specific heat can be observed to decrease with the increase in concentration. The observation is in agreement with the data shown in Fig. 9 along with the values drawn with Eq. (53) which is based on the law of mixtures.

The variation of density with temperature for different concentrations of Al₂O₃ (44 nm)/EG–water nanofluid is shown in Fig. 10. The density of nanofluid increases with concentration. However, the decrease in density with nanofluid temperature is not significant.

Fig. 10 Comparison of experimental values of density with mixture equation for different concentrations



7 Conclusions

The following conclusions are drawn from the present study:

- The nanofluid viscosity is significantly influenced by concentration, temperature, and particle size.
- The experimental data of viscosity reported by different authors deviate by more than 30 % for certain nanofluids.
- The Eqs. (23) and (24) developed with the aid of experimental data can be used to determine the viscosity of metal and oxide nanofluids.
- The thermal conductivity of nanofluid is dependent on volume fraction, particle diameter, and temperature of the nanofluid. The nanofluid thermal conductivity increases with volume fraction or concentration and temperature.
- Most of the authors reported an increase in thermal conductivity with the decrease in particle size
- The Eqs. (51) and (52) can be used to determine the thermal conductivity of metal and oxide nanofluids.
- The thermal diffusivity term in Eq. (52) distinguishes the material effects on nanofluid thermal conductivity. The equation can predict the thermal conductivity with a maximum deviation of 10 % for most metal and oxide nanofluids.
- The Eqs. (53) and (58) can be used to determine the specific heat and density of nanofluids, respectively.

Acknowledgments The authors acknowledge the financial assistance from the Ministry of Higher Education, Malaysia under FRGS grant vide Reference No. FRGS/1/2014/TK01/UTP/01/1 with cost centre 0153AB-K01.

References

- ASHRAE, A. (2005). *Handbook of fundamentals*. Atlanta, GA: American Society of Heating Refrigerating and Air Conditioning Engineers.
- Barbés, B., Páramo, R., Blanco, E., Pastoriza-Gallego, M. J., Piñeiro, M. M., Legido, J. L., et al. (2013). Thermal conductivity and specific heat capacity measurements of Al₂O₃ nanofluids. *Journal of Thermal Analysis and Calorimetry*, 111(2), 1615–1625.
- Batchelor, G. K. (1977). Effect of Brownian-motion on bulk stress in a suspension of spherical-particles. *Journal of Fluid Mechanics*, 83(1), 97–117.
- Beck, M. P., Yuan, Y., Warriar, P., & Teja, A. S. (2009). The effect of particle size on the thermal conductivity of alumina nanofluids. *Journal of Nanoparticle Research*, 11(5), 1129–1136.
- Beck, M. P., Yuan, Y., Warriar, P., & Teja, A. S. (2010). The thermal conductivity of alumina nanofluids in water, ethylene glycol, and ethylene glycol + water mixtures. *Journal of Nanoparticle Research*, 12(4), 1469–1477.
- Branson, B. T., Beauchamp, P. S., Beam, J. C., Lukehart, C. M., & Davidson, J. L. (2013). Nanodiamond nanofluids for enhanced thermal conductivity. *ACS Nano*, 7(4), 3183–3189.
- Brinkman, H. C. (1952). The viscosity of concentrated suspensions and solutions. *Journal of Chemical Physics*, 20(4), 571–581.
- Bruggeman, D. A. G. (1935). Berechnung verschiedener physikalischer konstanten von heterogenen substanzen. I. Dielektrizitätskonstanten und Leitfähigkeiten der mischkörper aus isotropen substanzen. *Annalen der Physik*, 24, 636–679.
- Buongiorno, J., Venerus, D. C., Prabhat, N., McKrell, T., Townsend, J., Christianson, R., et al. (2009). A benchmark study on the thermal conductivity of nanofluids. *Journal of Applied Physics*, 106(9), 094312.
- Chen, H., Ding, Y., He, Y., & Tan, C. (2007). Rheological behaviour of ethylene glycol based titania nanofluids. *Chemical Physics Letters*, 444(4–6), 333–337.
- Chon, C. H., Kihm, K. D., Lee, S. P., & Choi, S. U. (2005) Empirical correlation finding the role of temperature and particle size for nanofluid (Al₂O₃) thermal conductivity enhancement. *Applied Physics Letters*, 87(15), 153107–153107–3.
- Corcione, M. (2011). Empirical correlating equations for predicting the effective thermal conductivity and dynamic viscosity of nanofluids. *Energy Conversion and Management*, 52(1), 789–793.
- Das, S. K., Choi, S. U., & Patel, H. E. (2006). Heat transfer in nanofluids—A review. *Heat Transfer Engineering*, 27(10), 3–19.
- Das, S. K., Putra, N., Thiesen, P., & Roetzel, W. (2003). Temperature dependence of thermal conductivity enhancement for nanofluids. *Journal of Heat Transfer*, 125(4), 567–574.
- De Noni Jr, A., Garcia, D. E., & Hotza, D. (2002). A modified model for the viscosity of ceramic suspensions. *Ceramics International*, 28(7), 731–735.
- Duangthongsuk, W., & Wongwises, S. (2009). Measurement of temperature-dependent thermal conductivity and viscosity of TiO₂–water nanofluids. *Experimental Thermal and Fluid Science*, 33(4), 706–714.
- Eastman, J., Choi, S., Li, S., Yu, W., & Thompson, L. (2001). Anomalously increased effective thermal conductivities of ethylene glycol-based nanofluids containing copper nanoparticles. *Applied Physics Letters*, 78(6), 718–720.
- Every, A., Tzou, Y., Hasselman, D., & Raj, R. (1992). The effect of particle size on the thermal conductivity of ZnS/diamond composites. *Acta Metallurgica et Materialia*, 40(1), 123–129.
- Feng, Y., Yu, B., Feng, K., Xu, P., & Zou, M. (2008). Thermal conductivity of nanofluids and size distribution of nanoparticles by Monte Carlo simulations. *Journal of Nanoparticle Research*, 10(8), 1319–1328.
- Frankel, N. A., & Acrivos, A. (1967). On the viscosity of a concentrated suspension of solid spheres. *Chemical Engineering Science*, 22(6), 847–853.
- Fullman, R. (1953). *Measurement of particle sizes in opaque bodies*. General Electric Research Laboratory.

- Garg, J., Poudel, B., Chiesa, M., Gordon, J., Ma, J., Wang, J., et al. (2008). Enhanced thermal conductivity and viscosity of copper nanoparticles in ethylene glycol nanofluid. *Journal of Applied Physics*, 103(7), 074301.
- Ghadimi, A., Saidur, R., & Metselaar, H. (2011). A review of nanofluid stability properties and characterization in stationary conditions. *International Journal of Heat and Mass Transfer*, 54(17), 4051–4068.
- Godson, L., Raja, B., Lal, D. M., & Wongwises, S. (2010). Experimental investigation on the thermal conductivity and viscosity of silver-deionized water nanofluid. *Experimental Heat Transfer*, 23(4), 317–332.
- Graham, A. L. (1981). On the viscosity of suspensions of solid spheres. *Applied Scientific Research*, 37(3), 275–286.
- Hagen, K. D. (1999). *Heat transfer with applications*. : Prentice Hall.
- Hamilton, R. L., & Crosser, O. K. (1962). Thermal conductivity of heterogeneous two-component systems. *Industrial and Engineering Chemistry Fundamentals*, 1(3), 182–191.
- He, Y., Jin, Y., Chen, H., Ding, Y., Cang, D., & Lu, H. (2007). Heat transfer and flow behaviour of aqueous suspensions of TiO₂ nanoparticles (nanofluids) flowing upward through a vertical pipe. *International Journal of Heat and Mass Transfer*, 50(11), 2272–2281.
- Hwang, Y., Lee, J. K., Lee, C. H., Jung, Y. M., Cheong, S. I., Lee, C. G., et al. (2007). Stability and thermal conductivity characteristics of nanofluids. *Thermochimica Acta*, 455(1–2), 70–74.
- Jang, S. P., & Choi, S. U. (2004). Role of Brownian motion in the enhanced thermal conductivity of nanofluids. *Applied Physics Letters*, 84(21), 4316–4318.
- Jang, S. P., & Choi, S. U. (2007). Effects of various parameters on nanofluid thermal conductivity. *Journal of Heat Transfer*, 129(5), 617–623.
- Kakaç, S., & Pramuanjaroenkij, A. (2009). Review of convective heat transfer enhancement with nanofluids. *International Journal of Heat and Mass Transfer*, 52(13–14), 3187–3196.
- Karthikeyan, N. R., Philip, J., & Raj, B. (2008). Effect of clustering on the thermal conductivity of nanofluids. *Materials Chemistry and Physics*, 109(1), 50–55.
- Kazemi-Beydokhti, A., Heris, S. Z., Moghadam, N., Shariati-Niasar, M., & Hamidi, A. A. (2014). Experimental investigation of parameters affecting nanofluid effective thermal conductivity. *Chemical Engineering Communications*, 201(5), 593–611.
- Kebllinski, P., Phillpot, S. R., Choi, S. U. S., & Eastman, J. A. (2002). Mechanisms of heat flow in suspensions of nano-sized particles (nanofluids). *International Journal of Heat and Mass Transfer*, 45(4), 855–863.
- Khanafar, K., & Vafai, K. (2011). A critical synthesis of thermophysical characteristics of nanofluids. *International Journal of Heat and Mass Transfer*, 54(19), 4410–4428.
- Kim, S. H., Choi, S. R., & Kim, D. (2007). Thermal conductivity of metal-oxide nanofluids: Particle size dependence and effect of laser irradiation. *Journal of Heat Transfer*, 129(3), 298–307.
- Kitano, T., Kataoka, T., & Shiota, T. (1981). An empirical equation of the relative viscosity of polymer melts filled with various inorganic fillers. *Rheologica Acta*, 20(2), 207–209.
- Kleinstreuer, C., & Feng, Y. (2011). Experimental and theoretical studies of nanofluid thermal conductivity enhancement: A review. *Nanoscale Research Letters*, 6(1), 439.
- Kole, M., & Dey, T. K. (2010). Thermal conductivity and viscosity of Al₂O₃ nanofluid based on car engine coolant. *Journal of Physics. D. Applied Physics*, 43, 315501.
- Koo, J., & Kleinstreuer, C. (2004). A new thermal conductivity model for nanofluids. *Journal of Nanoparticle Research*, 6(6), 577–588.
- Koo, J., & Kleinstreuer, C. (2005). Impact analysis of nanoparticle motion mechanisms on the thermal conductivity of nanofluids. *International Communications in Heat and Mass Transfer*, 32(9), 1111–1118.
- Krieger, I. M., & Dougherty, T. J. (1959). A mechanism for non-newtonian flow in suspensions of rigid spheres. *Transactions of The Society of Rheology*, 3(1), 137–152.
- Kulkarni, D. P., Das, D. K., & Chukwu, G. A. (2006). Temperature dependent rheological property of copper oxide nanoparticles suspension (nanofluid). *Journal of Nanoscience and Nanotechnology*, 6(4), 1150–1154.

- Kulkarni, D. P., Das, D. K., & Patil, S. L. (2007). Effect of temperature on rheological properties of copper oxide nanoparticles dispersed in propylene glycol and water mixture. *Journal of Nanoscience and Nanotechnology*, 7(7), 2318–2322.
- Kulkarni, D. P., Namburu, P. K., Ed Bargar, H., & Das, D. K. (2008). Convective heat transfer and fluid dynamic characteristics of SiO₂ ethylene glycol/water nanofluid. *Heat Transfer Engineering*, 29(12), 1027–1035.
- Lee, J.-H., Hwang, K. S., Jang, S. P., Lee, B. H., Kim, J. H., Choi, S. U. S., et al. (2008). Effective viscosities and thermal conductivities of aqueous nanofluids containing low volume concentrations of Al₂O₃ nanoparticles. *International Journal of Heat and Mass Transfer*, 51(11–12), 2651–2656.
- Lee, J.-H., Lee, S.-H., Choi, C. J., Jang, S. P., & Choi, S. U. (2010). A review of thermal conductivity data, mechanisms and models for nanofluids. *International Journal of Micro-Nano Scale Transport*, 1(4), 269–322.
- Lee, S., Choi, S.-S., Li, S., & Eastman, J. (1999). Measuring thermal conductivity of fluids containing oxide nanoparticles. *Journal of Heat Transfer*, 121(2), 280–289.
- Leong, K. C., Yang, C., & Murshed, S. M. S. (2006). A model for the thermal conductivity of nanofluids—The effect of interfacial layer. *Journal of Nanoparticle Research*, 8(2), 245–254.
- Li, C. H., & Peterson, G. (2006). Experimental investigation of temperature and volume fraction variations on the effective thermal conductivity of nanoparticle suspensions (nanofluids). *Journal of Applied Physics*, 99(8), 084314.
- Li, J., Li, Z., & Wang, B. (2002). Experimental viscosity measurements for copper oxide nanoparticle suspensions. *Tsinghua Science and Technology*, 7(2), 198–201.
- Li, X. F., Zhu, D. S., Wang, X. J., Wang, N., Gao, J. W., & Li, H. (2008). Thermal conductivity enhancement dependent pH and chemical surfactant for Cu–H₂O nanofluids. *Thermochimica Acta*, 469(1–2), 98–103.
- Lundgren, T. S. (1972). Slow flow through stationary random beds and suspensions of spheres. *Journal of Fluid Mechanics*, 51(02), 273–299.
- Mahbulbul, I., Saidur, R., & Amalina, M. (2012). Latest developments on the viscosity of nanofluids. *International Journal of Heat and Mass Transfer*, 55(4), 874–885.
- Mahian, O., Kianifar, A., & Wongwises, S. (2013). Dispersion of ZnO nanoparticles in a mixture of ethylene glycol–water, exploration of temperature-dependent density, and sensitivity analysis. *Journal of Cluster Science*, 24(4), 1103–1114.
- Mariano, A., Pastoriza-Gallego, M. J., Lugo, L., Camacho, A., Canzonieri, S., & Piñeiro, M. M. (2013). Thermal conductivity, rheological behaviour and density of non-Newtonian ethylene glycol-based SnO₂ nanofluids. *Fluid Phase Equilibria*, 337, 119–124.
- Masuda, H., Ebata, A., Teramae, K., & Hishinuma, N. (1993). Alteration of thermal conductivity and viscosity of liquid by dispersing ultra-fine particles. *Netsu Bussei*, 7(4), 227–233.
- Maxwell, J.C. (1881). *Treatise on electricity and magnetism* (2nd ed.). Oxford, UK: Clarendon Press.
- Mintsa, H. A., Roy, G., Nguyen, C. T., & Doucet, D. (2009). New temperature dependent thermal conductivity data for water-based nanofluids. *International Journal of Thermal Sciences*, 48(2), 363–371.
- Mishra, P. C., Mukherjee, S., Nayak, S. K., & Panda, A. (2014). A brief review on viscosity of nanofluids. *International Nano Letters*, 4(4), 109–120.
- Murshed, S. M. S. (2011a). Simultaneous measurement of thermal conductivity, thermal diffusivity, and specific heat of nanofluids. *Heat Transfer Engineering*, 33(8), 722–731.
- Murshed, S. M. S., Leong, K. C., & Yang, C. (2005). Enhanced thermal conductivity of TiO₂–water based nanofluids. *International Journal of Thermal Sciences*, 44(4), 367–373.
- Murshed, S. M. S., Leong, K. C., & Yang, C. (2008). Investigations of thermal conductivity and viscosity of nanofluids. *International Journal of Thermal Sciences*, 47(5), 560–568.
- Murshed, S. M. S., Leong, K. C., & Yang, C. (2009). A combined model for the effective thermal conductivity of nanofluids. *Applied Thermal Engineering*, 29(11–12), 2477–2483.
- Murshed, S. S. (2011b). Determination of effective specific heat of nanofluids. *Journal of Experimental Nanoscience*, 6(5), 539–546.

- Namburu, P., Kulkarni, D., Dandekar, A., & Das, D. (2007). Experimental investigation of viscosity and specific heat of silicon dioxide nanofluids. *Micro and Nano Letters, IET*, 2(3), 67–71.
- Nguyen, C. T., Desgranges, F., Roy, G., Galanis, N., Maré, T., Boucher, S., et al. (2007). Mints, temperature and particle-size dependent viscosity data for water-based nanofluids—Hysteresis phenomenon. *International Journal of Heat and Fluid Flow*, 28(6), 1492–1506.
- Nielsen, L. E. (1970). Generalized equation for the elastic moduli of composite materials. *Journal of Applied Physics*, 41(11), 4626–4627.
- Özeringç, S., Kakaç, S., & Yazıcıoğlu, A. G. (2010). Enhanced thermal conductivity of nanofluids: A state-of-the-art review. *Microfluidics and Nanofluidics*, 8(2), 145–170.
- Pak, B. C., & Cho, Y. I. (1998). Hydrodynamic and heat transfer study of dispersed fluids with submicron metallic oxide particles. *Experimental Heat Transfer an International Journal*, 11(2), 151–170.
- Patel, H. E., Sundararajan, T., & Das, S. K. (2010). An experimental investigation into the thermal conductivity enhancement in oxide and metallic nanofluids. *Journal of Nanoparticle Research*, 12(3), 1015–1031.
- Prasher, R., Phelan, P. E., & Bhattacharya, P. (2006a). Effect of aggregation kinetics on the thermal conductivity of nanoscale colloidal solutions (nanofluid). *Nano Letters*, 6(7), 1529–1534.
- Prasher, R., Song, D., Wang, J., & Phelan, P. (2006b). Measurements of nanofluid viscosity and its implications for thermal applications. *Applied Physics Letters*, 89(13), 133108.
- Sahoo, B. C., Das, D. K., Vajjha, R. S., & Satti, J. R. (2012). Measurement of the thermal conductivity of silicon dioxide nanofluid and development of correlations. *Journal of Nanotechnology in Engineering and Medicine*, 3(4), 041006.
- Sekhar, Y. R., & Sharma, K. (2015). Study of viscosity and specific heat capacity characteristics of water-based Al_2O_3 nanofluids at low particle concentrations. *Journal of Experimental Nanoscience*, 10(2), 86–102.
- Sharma, A. K., Tiwari, A. K., & Dixit, A. R. (2016). Rheological behaviour of nanofluids: A review. *Renewable and Sustainable Energy Reviews*, 53, 779–791.
- Sharma, K., Sarma, P., Azmi, W., Mamat, R., & Kadrigama, K. (2010). Correlations to predict friction and forced convection heat transfer coefficients of water based nanofluids for turbulent flow in a tube. *International Journal of Microscale and Nanoscale Thermal and Fluid Transport Phenomena*, 3, 283–308.
- Shima, P., Philip, J., & Raj, B. (2009). Role of microconvection induced by Brownian motion of nanoparticles in the enhanced thermal conductivity of stable nanofluids. *Applied Physics Letters*, 94(22), 223101.
- Sridhara, V., & Satapathy, L. N. (2011). Al_2O_3 -based nanofluids: A review. *Nanoscale Research Letters*, 6(1), 1–16.
- Sun, T., & Teja, A. S. (2004). Density, viscosity and thermal conductivity of aqueous solutions of propylene glycol, dipropylene glycol, and tripropylene glycol between 290 K and 460 K. *Journal of Chemical and Engineering Data*, 49(5), 1311–1317.
- Sundar, L. S., Ramana, E. V., Singh, M. K., & Sousa, A. C. (2014). Thermal conductivity and viscosity of stabilized ethylene glycol and water mixture Al_2O_3 nanofluids for heat transfer applications: an experimental study. *International Communications in Heat and Mass Transfer*, 56, 86–95.
- Sundar, L. S., Sharma, K., Naik, M., & Singh, M. K. (2013a). Empirical and theoretical correlations on viscosity of nanofluids: A review. *Renewable and Sustainable Energy Reviews*, 25, 670–686.
- Sundar, L. S., Singh, M. K., & Sousa, A. C. (2013b). Thermal conductivity of ethylene glycol and water mixture based Fe_3O_4 nanofluid. *International Communications in Heat and Mass Transfer*, 49, 17–24.
- Teng, T.-P., & Hung, Y.-H. (2014). Estimation and experimental study of the density and specific heat for alumina nanofluid. *Journal of Experimental Nanoscience*, 9(7), 707–718.

- Teng, T.-P., Hung, Y.-H., Teng, T.-C., Mo, H.-E., & Hsu, H.-G. (2010). The effect of alumina/water nanofluid particle size on thermal conductivity. *Applied Thermal Engineering*, 30(14), 2213–2218.
- Tseng, W. J., & Lin, K.-C. (2003). Rheology and colloidal structure of aqueous TiO₂ nanoparticle suspensions. *Materials Science and Engineering A*, 355(1–2), 186–192.
- Turgut, A., Tavman, I., Chirtoc, M., Schuchmann, H. P., Sauter, C., & Tavman, S. (2009). Thermal conductivity and viscosity measurements of water-based TiO₂ nanofluids. *International Journal of Thermophysics*, 30, 1213–1226.
- Vajjha, R., Das, D., & Mahagaonkar, B. (2009). Density measurement of different nanofluids and their comparison with theory. *Petroleum Science and Technology*, 27(6), 612–624.
- Vajjha, R. S., & Das, D. K. (2009a). Experimental determination of thermal conductivity of three nanofluids and development of new correlations. *International Journal of Heat and Mass Transfer*, 52(21), 4675–4682.
- Vajjha, R. S., & Das, D. K. (2009b). Specific heat measurement of three nanofluids and development of new correlations. *Journal of Heat Transfer*, 131(7), 071601.
- Wang, B.-X., Zhou, L.-P., & Peng, X.-F. (2006). Surface and size effects on the specific heat capacity of nanoparticles. *International Journal of Thermophysics*, 27(1), 139–151.
- Wang, X., Xu, X., & Choi, S. U. S. (1999). Thermal conductivity of nanoparticle–fluid mixture. *Journal of Thermophysics and Heat Transfer*, 13(4), 474–480.
- Wang, X.-J., Zhu, D.-S., & Yang, S. (2009). Investigation of pH and SDBS on enhancement of thermal conductivity in nanofluids. *Chemical Physics Letters*, 470(1–3), 107–111.
- Wang, X.-Q., & Mujumdar, A. S. (2007). Heat transfer characteristics of nanofluids: A review. *International Journal of Thermal Sciences*, 46(1), 1–19.
- Wang, Y., Fisher, T. S., Davidson, J., & Jiang, L. (2002). Thermal conductivity of nanoparticle suspensions. In *8th AIAA and ASME Joint Thermophysics and Heat Transfer Conference*.
- Wasp, F. J. (1977). *Solid-liquid slurry pipeline transportation*. Berlin: Trans. Tech.
- White, F. M. (1991). *Viscous fluid flow*.
- Xie, H., Fujii, M., & Zhang, X. (2005). Effect of interfacial nanolayer on the effective thermal conductivity of nanoparticle–fluid mixture. *International Journal of Heat and Mass Transfer*, 48(14), 2926–2932.
- Xie, H., Wang, J., Xi, T., & Liu, Y. (2001). Study on the thermal conductivity of SiC nanofluids. *Journal-Chinese Ceramic Society*, 29(4), 361–364.
- Xie, H., Wang, J., Xi, T., Liu, Y., Ai, F., & Wu, Q. (2002a). Thermal conductivity enhancement of suspensions containing nanosized alumina particles. *Journal of Applied Physics*, 91(7), 4568–4572.
- Xie, H., Yu, W., & Chen, W. (2010). MgO nanofluids: Higher thermal conductivity and lower viscosity among ethylene glycol-based nanofluids containing oxide nanoparticles. *Journal of Experimental Nanoscience*, 5(5), 463–472.
- Xie, H., Yu, W., Li, Y., & Chen, L. (2011). Discussion on the thermal conductivity enhancement of nanofluids. *Nanoscale Research Letters*, 6(1), 124.
- Xie, H.-Q., Wang, J.-C., Xi, T.-G., & Liu, Y. (2002b). Thermal conductivity of suspensions containing nanosized SiC particles. *International Journal of Thermophysics*, 23(2), 571–580.
- Xuan, Y., & Li, Q. (2000). Heat transfer enhancement of nanofluids. *International Journal of Heat and Fluid Flow*, 21(1), 58–64.
- Xue, Q., & Xu, W.-M. (2005). A model of thermal conductivity of nanofluids with interfacial shells. *Materials Chemistry and Physics*, 90(2), 298–301.
- Xue, Q.-Z. (2003). Model for effective thermal conductivity of nanofluids. *Physics Letters A*, 307(5), 313–317.
- Yiamsawasdi, T., Dalkilic, A. S., & Wongwises, S. (2012). Measurement of specific heat of nanofluids. *Current Nanoscience*, 8(6), 939–944.
- Yoo, D.-H., Hong, K., & Yang, H.-S. (2007). Study of thermal conductivity of nanofluids for the application of heat transfer fluids. *Thermochimica Acta*, 455(1), 66–69.
- Yu, C. J., Richter, A., Datta, A., Durbin, M., & Dutta, P. (2000). Molecular layering in a liquid on a solid substrate: an X-ray reflectivity study. *Physica B: Condensed Matter*, 283(1), 27–31.

- Yu, W., & Choi, S. (2004). The role of interfacial layers in the enhanced thermal conductivity of nanofluids: a renovated Hamilton-Crosser model. *Journal of Nanoparticle Research*, 6(4), 355–361.
- Yu, W., & Choi, S. U. S. (2003). The role of interfacial layers in the enhanced thermal conductivity of nanofluids: A renovated Maxwell model. *Journal of Nanoparticle Research*, 5 (1–2), 16–171.
- Yu, W., Xie, H., Li, Y., Chen, L., & Wang, Q. (2012). Experimental investigation on the heat transfer properties of Al₂O₃ nanofluids using the mixture of ethylene glycol and water as base fluid. *Powder Technology*, 230, 14–19.
- Zhou, L.-P., Wang, B.-X., Peng, X.-F., Du, X.-Z., & Yang, Y.-P. (2010) On the specific heat capacity of CuO nanofluid. *Advances in Mechanical Engineering*.
- Zhou, S.-Q., & Ni, R. (2008). Measurement of the specific heat capacity of water-based Al₂O₃ nanofluid. *Applied Physics Letters*, 92(9), 093123–093123–3.
- Zhu, H., Zhang, C., Liu, S., Tang, Y., & Yin, Y. (2006). Effects of nanoparticle clustering and alignment on thermal conductivities of Fe₃O₄ aqueous nanofluids. *Applied Physics Letters*, 89 (2), 3123.